Dear Dr. Brook (Co-Editor):

We are submitting a revised paper (manuscript #acp-2017-1091) entitled, *Emissions databases for polycyclic aromatic compounds in the Canadian Athabasca Oil Sands Region – development using current knowledge and evaluation with passive sampling and air dispersion modelling data*, for further consideration in Atmospheric Chemistry and Physics. We have addressed all of the comments provided by the three reviewers. The details can be found in the enclosed response to reviewers' comments. For your convenience, a copy of the paper with track changes is also enclosed.

Thank you for taking care of the review process for this paper.

Sincerely,

Xin Qiu, Irene Cheng, Fuquan Yang, Erin Horb, Leiming Zhang, and Tom Harner

Response to Reviewers' Comments

Emissions databases for polycyclic aromatic compounds in the Canadian Athabasca Oil Sands Region – development using current knowledge and evaluation with passive sampling and air dispersion modelling data (acp-2017-1091)

Referee #1

We appreciate the comments by the reviewer to help us improve the paper. Our responses to the specific comments are shown below in blue.

This paper developed two speciated and spatially-resolved emissions databases for polycyclic aromatic compounds (PAC) in the Athabasca oil sands region (AOSR), and compared the two emissions databases with the measurements from a passive air monitoring network. Papers have a high degree of novelty and I recommend to publish after a minor revised.

1. Please delete some basic concepts, concise articles.

Response: We condensed and deleted some of the basic information (e.g. basics about PAHs in the first paragraph of the introduction) in the revised paper to keep it concise.

2. What are the PAHs in CEMA database and JOSM database, respectively? Are they the same?

Response: The 16 parent PAHs are the same in the CEMA-derived and JOSM-derived emissions databases. As mentioned in sect. 2.2, the PAHs include: naphthalene (NAPH), acenaphthylene (ACY), acenaphthene (ACE), fluorene (FLR), phenanthrene (PHEN), anthracene (ANTH), fluoranthene (FLRT), pyrene (PYR), benz[a]anthracene (BaA), coeluting chrysene and triphenylene (CHRYþTRIP), benzo[b]fluoranthene (BbF), benzo[k]fluoranthene (BkF), benzo[a]pyrene (BaP), indeno[1,2,3-cd]pyrene (I123cdP), dibenz[a,h]anthracene (dBahA) and benzo[ghi]perylene (BghiP). However, total alkylated PAHs and dibenzothiophenes (DBT) concentrations were modelled for the JOSM-derived emissions scenario only, since the monitoring of these additional compounds is part of monitoring activities under the JOSM program. This is clarified in sect. 2.2 (2nd paragraph) of the revised paper.

3. In Results and Discussion, please describe the same meteorological data in detail.

Response: A more detailed description of the meteorological data input for the CALMET model is provided in sect. 2.2 (1st paragraph) of the revised paper.

CALPUFF takes three-dimensionally varying wind, temperature and turbulence fields from the CALMET model. The 3-D winds and temperature fields from CALMET are reconstructed using meteorological measurements, orography and land use data. Besides wind and temperature fields, CALMET determines the 2-D fields of micrometeorological variables needed to carry out dispersion simulations (mixing height, Monin Obukhov length, friction velocity, convective velocity, etc.). A two-step approach is typically used to compute the wind fields in CALMET.

In the first step, an initial guess wind field is adjusted for kinematic effects of terrain, slope flows, and terrain blocking effects. The second step applies an objective analysis procedure to introduce observational data into the first step to produce the final wind fields. In this study, CALMET used the Weather Research and Forecasting (WRF) model due to its capability of simulating regional flows and certain aspects of local meteorological conditions such as complex terrain. It replaces the two-step approach given the higher spatial resolution of the WRF output compared to observational data. The output of the CALMET model is directly interfaced with the CALPUFF dispersion model for further air quality modelling.

Referee #2

We appreciate the comments by the reviewer to help us improve the paper. Our responses to the specific comments are shown below in blue.

Within the article, two speciated and spatially-resolved emissions databases for PACs in AOSR were developed. Further, the PAC concentrations in AOSR were simulated using the CALPUFF atmospheric dispersion model for both scenarios (both databases) and compared with passive monitoring data to assess which emissions input can achieve better agreement with measurements. According to my opinion, the manuscript represent a significant scientific contribution in studying PACs (PAHs, alkylated PAHS and DBTs) in oil sends regions where uncertainties in the PACs emissions are still significant. I recommend the manuscript for publication with minor revision:

1. Although if deposition had been considered in the CALPUFF model, the modeled values would be even lower then the measured, I would ask the authors to explain why they have excluded the loss by wet and dry deposition in the modeling process. Were there any other reasons?

Response: We made this decision after running a few model scenarios and decided to present the model results without deposition processes. This is because modeled concentrations from simulating emissions, transport and dispersion processes, but without deposition processes, are already lower than measurements, demonstrating that emission inputs are conservative or underestimated. By including deposition processes, modeled concentrations would be even lower than measurements; however, in this model scenario it would be hard to say if this was caused by too low emissions input or too high deposition rates, knowing that large uncertainties exist in treating dry and wet deposition processes. For example, there are large uncertainties in the PAC dry deposition velocities (Zhang et al., 2015a), PAC scavenging ratios for snow and rain scavenging of gas-phase and particulate-phase PACs (Zhang et al., 2015b), and scavenging coefficients of aerosols in general by snow and rain scavenging processes (Zhang et al., 2013; Wang et al., 2014). Our rationale for excluding deposition loss in the model is discussed in the paragraph before sect. 3.3 of the revised paper. In our next study related to this project, we plan on comparing the deposition output using various approaches.

2. The authors should also take into consideration the fact that values of PAC concentrations obtained using the passive samplers refer only to the gaseous phase of pollutant and reflect a more accurate concentration for the low molecular weight PACs compering to high molecular weight compounds.

Response: Although certain types of passive air samplers show a bias for gas-phase compounds, the PUF disk samplers used in the oil sands network have been shown to capture both gas-phase and particle-phase PAHs with the same efficiency as conventional high volume air samplers (Harner et al., 2013; Markovic et al., 2015).

References:

Harner, T., Su, K., Genualdi, S., Karpowicz, J., Ahrens, L., Mihele, C., Schuster, J., Charland, J. -P. and Narayan, J.: Calibration and application of PUF disk passive air samplers for tracking polycyclic aromatic compounds (PACs), Atmos. Environ., 75, 123-128, 2013.

Markovic, M., Prokop, S., Staebler, R.M., Liggio, J., Harner, T: Evaluation of the particle infiltration efficiency of three passive samplers and the PS-1 active air sampler, Atmos. Environ., 112, 289-293, 2015.

Wang, X., Zhang, L., and Moran, M. D.: Development of a new semi-empirical parameterization for below-cloud scavenging of size-resolved aerosol particles by both rain and snow, Geosci. Model Dev., 7, 799-819, 2014.

Zhang, L., Cheng, I., Wu, Z., Harner, T., Schuster, J., Charland, J. P., Muir, D., and Parnis, J.M.: Dry deposition of PACs to various land covers in the Athabasca Oil Sands Region, J. Adv. Model. Earth Sy., 7, 1339-1350, 2015a.

Zhang, L., Cheng, I., Muir, D., and Charland, J.-P.: Scavenging ratios of polycyclic aromatic compounds in rain and snow in the Athabasca oil sands region, Atmos. Chem. Phys., 15, 1421-1434, 2015b.

Zhang, L., Wang, X., Moran, M. D., and Feng, J.: Review and uncertainty assessment of size-resolved scavenging coefficient formulations for below-cloud snow scavenging of atmospheric aerosols, Atmos. Chem. Phys., 13, 10005-10025, 2013.

Referee #3

We appreciate the comments by the reviewer to help us improve the paper. Our responses to the specific comments are shown below in blue.

This research work compared CALPUFF modelling results applying the two air emissions databases of CEMA and JOSM programs. The modelling results are then compared with observations to evaluate accuracy of the air emissions values. This research makes significant contribution to the work of PAHs air emission estimation in the oil sands region. While dispersion models could have systematic error existing inherently in the model, particularly and usually lead to underestimation at low pollutant concentrations, this research presents a progressive approach to compare the modelling results relatively for the original emissions data and the improved one. I suggest to publish it to make colleagues working in this field be aware of the work progress.

It would be clearer if the author could add more information on meteorology and emission summary.

Response: A summary of the meteorological model that drives the CALPUFF model is provided in sect. 2.2 (1st paragraph) of the revised paper. CALPUFF takes three-dimensionally varying wind, temperature and turbulence fields from the CALMET model. The 3-D winds and temperature fields from CALMET are reconstructed using meteorological measurements, orography and land use data. Besides wind and temperature fields, CALMET determines the 2-D fields of micrometeorological variables needed to carry out dispersion simulations (mixing height, Monin Obukhov length, friction velocity, convective velocity, etc.). A two-step approach is typically used to compute the wind fields in CALMET. In the first step, an initial guess wind field is adjusted for kinematic effects of terrain, slope flows, and terrain blocking effects. The second step applies an objective analysis procedure to introduce observational data into the first step to produce the final wind fields. In this study, CALMET used the Weather Research and Forecasting (WRF) model due to its capability of simulating regional flows and certain aspects of local meteorological conditions such as complex terrain. It replaces the two-step approach given the higher spatial resolution of the WRF output compared to observational data. The output of the CALMET model is directly interfaced with the CALPUFF dispersion model for further air quality modelling.

A paragraph summarizing the PAC emissions is included in sect 3.1 of the revised paper and also provided below. We also added a map showing the spatial distribution of the unsubstituted PAH emissions in Fig. S3 of the Supplement.

3.1 PAC emissions estimates

Over the model domain, the total unsubstituted PAH emissions (2009-2014) are estimated to be 56 to 58 tonnes yr^{-1} based on emissions from tailings ponds, mine face, mine fleet, residential, commercial, local traffic, airport, point, and transportation sources (Table 1). A map of the spatial distribution of the emissions is shown in Fig. S3 of the Supplement. Point sources accounted for most of the total unsubstituted PAH emissions (75-77%). The major difference in the total unsubstituted PAH emissions between the CEMA-derived and JOSM-derived emissions databases is the higher evaporative PAH emissions from tailings ponds and mine face in the JOSM-derived emissions database. Alkylated PAH and DBT emissions (2011-2014) are estimated to be 17 tonnes yr^{-1} and 0.26 tonnes yr^{-1} respectively; however, they consisted of fewer emission sources (tailings ponds, mine fleet and transportation sources) due to a lack of PAC speciation data to estimate these emissions. Nevertheless, the PAC emissions estimates may still be underestimated from oil sands sources, such as tailings ponds and fugitive dust. Recent studies suggest that flux chamber measurements of tailings pond emissions underestimate organic compound emission fluxes (Tran et al., 2018). Windblown petcoke dust observed recently over surface mining areas in the AOSR (Zhang et al., 2016) also have not been accounted for in the PAC emissions databases. In addition to gaps in the existing emissions databases, speciation profiles were largely missing particularly for alkylated PAHs and DBTs. In this paper, the focus is on unsubstituted PAHs; however, alkylated PAHs and DBTs were still modelled despite the limited knowledge of the emissions profiles.

Additionally, PAHs have a wide spectrum including compounds in gaseous phase and particulate phase, which can exhibit different characteristics during transport and deposition. Although the research is focused on relative comparison of two emissions databases with only considering dispersion, the author may analyze qualitatively the resultant impact of turning off deposition modelling on modelling results in general.

Response: We decided to present the model results without deposition processes after running a few model scenarios. One of the impacts of turning off deposition modelling is that the modelled air concentrations are higher compared to those with deposition modelling turned on. However, we found that the modeled concentrations from simulating emission, transport and dispersion processes, but without deposition processes, are already lower than measurements, demonstrating that the emissions inputs are conservative or underestimated. If deposition processes were included, modeled concentrations would be even lower than measurements; however, in this model scenario it would be hard to say if this was caused by too low emissions input or too high deposition rates, knowing that large uncertainties exist in treating dry and wet deposition processes. For example, there are large uncertainties in the PAC dry deposition velocities (Zhang et al., 2015a), PAC scavenging ratios for snow and rain scavenging of gas-phase and particulate-phase PACs (Zhang et al., 2015b), and scavenging coefficients of aerosols in general by snow and rain scavenging processes (Zhang et al., 2013; Wang et al., 2014). This discussion is provided in the paragraph before sect. 3.3 of the revised paper. In our next study related to this project, we plan on comparing the deposition output using various approaches.

References:

Tran, H. N. Q., Lyman, S. N., Mansfield, M. L., O'Neil, T., Bowers, R. L., Smith, A. P. and Keslar, C.: Emissions of Organic Compounds from Produced Water Ponds II: Evaluation of flux-chamber measurements with inverse-modeling techniques, J. Air Waste Manag. Assoc., DOI: 10.1080/10962247.2018.1426654, 2018.

Wang, X., Zhang, L., and Moran, M. D.: Development of a new semi-empirical parameterization for below-cloud scavenging of size-resolved aerosol particles by both rain and snow, Geosci. Model Dev., 7, 799-819, 2014.

Zhang, L., Cheng, I., Wu, Z., Harner, T., Schuster, J., Charland, J. P., Muir, D., and Parnis, J.M.: Dry deposition of PACs to various land covers in the Athabasca Oil Sands Region, J. Adv. Model. Earth Sy., 7, 1339-1350, 2015a.

Zhang, L., Cheng, I., Muir, D., and Charland, J.-P.: Scavenging ratios of polycyclic aromatic compounds in rain and snow in the Athabasca oil sands region, Atmos. Chem. Phys., 15, 1421-1434, 2015b.

Zhang, L., Wang, X., Moran, M. D., and Feng, J.: Review and uncertainty assessment of size-resolved scavenging coefficient formulations for below-cloud snow scavenging of atmospheric aerosols, Atmos. Chem. Phys., 13, 10005-10025, 2013.

Zhang, Y., Shotyk, W., Zaccone, C., Noernberg, T., Pelletier, R., Bicalho, B., Froese, D. G., Davies, L. and Martin, J. W.: Airborne petcoke dust is a major source of polycyclic aromatic hydrocarbons in the Athabasca Oil Sands Region, Environ. Sci. Technol., 50(4), 1711-1720, 2016.

Emissions databases for polycyclic aromatic compounds in the Canadian Athabasca Oil Sands Region – development using current knowledge and evaluation with passive sampling and air dispersion modelling data

Xin Qiu[1], Irene Cheng[2], Fuquan Yang[1], Erin Horb[3], Leiming Zhang[2], Tom Harner[2]

[1]Novus Environmental Inc., Guelph, Ontario, N1G 4T2, Canada
[2]Air Quality Research Division, Science and Technology Branch, Environment and Climate Change Canada, Toronto, Ontario, M3H 5T4, Canada
[3]Novus Environmental Inc., Calgary, Alberta, T2R 1K7, Canada

Correspondence to: Xin Qiu (xinq@novusenv.com) and Leiming Zhang (leiming.zhang@canada.ca)

Abstract. Two speciated and spatially-resolved emissions databases for polycyclic aromatic compounds (PAC) in the Athabasca oil sands region (AOSR) were developed. The first database was derived from volatile organic compound (VOC) emissions data provided by the Cumulative Environmental Management Association (CEMA) and the second database was derived from additional data collected within the Joint Canada-Alberta Oil Sands Monitoring (JOSM) program. CALPUFF modelling results for atmospheric polycyclic aromatic hydrocarbons (PAH), alkylated PAH, and dibenzothiophenes (DBT), obtained using each of the emissions databases, are presented and compared with measurements from a passive air monitoring network. The JOSM-derived emissions resulted in better model-measurement agreement in the total PAH concentrations and for most PAH species concentrations, compared to results using CEMA-derived emissions. At local sites near oil sands mines, the percent error of the model compared to observations decreased from 30% using the CEMA-derived emissions to 17% using the JOSM-derived emissions. The improvement at local sites was likely attributed to the inclusion of updated tailings pond emissions estimated from JOSM activities. In either the CEMA-derived or JOSM-derived emissions scenario, the model underestimated PAH concentrations by a factor of 3 at remote locations. Potential reasons for the disagreement include forest fire emissions, re-emissions of previously deposited PAHs, and long-range transport not considered in the model. Alkylated PAH and DBT concentrations were also significantly underestimated. The CALPUFF model is expected to predict higher concentrations because of the limited chemistry and deposition modelling. Thus the model underestimation of PACs is likely due to gaps in the emissions database for these compounds and uncertainties in the methodology for estimating the emissions. Future work is required that focuses on improving the PAC emission estimation and speciation methodologies and reducing the uncertainties in VOC emissions which are subsequently used in PAC emissions estimation.

1 Introduction

Polycyclic aromatic compounds (PACs) ~~are a ubiquitous class of contaminants found naturally in geological deposits and produced as a byproduct of incomplete combustion of organic material (Baek et al., 1991; Boström et al., 2002; Neff et al., 2005). The broad PAC chemical classification includes hundreds of organic compounds that contain two or more fused benzene rings (Keyte et al., 2013; Kim et al., 2013). PACs~~ include not only unsubstituted polycyclic aromatic hydrocarbons (PAHs), which have been the focus of previous scientific investigations (Timoney and Lee, 2011; Jautzy et al., 2013; Galarneau et al., 2014a,b; Hsu et al., 2015), but also alkylated PAHs, ~~parent~~unsubstituted- and alkylated-dibenzothiophenes (DBTs) and other heterocyclic aromatic compounds containing nitrogen, sulphur or oxygen (Giesy et al., 2010; Schuster et al., 2015; Jariyasopit et al., 2016; Manzano et al., 2017). Exposure to some PACs has led to various carcinogenic~~, teratogenic and genotoxic effects in animals and humans and cases of skin and eye irritation and inflammation~~ and/or mutagenic effects (ATSDR, 2009; CCME, 2010; Kim et al., 2013; Wickliffe et al., 2014; Zhang et al., 2015a). ~~–~~Detailed toxicity information on individual PAC species have not been elucidated because subjects have mainly been exposed to a mixture of compounds (Gosselin et al., 2010; Kim et al., 2013; Jariyasopit et al., 2016). Limited toxicology data suggests some alkylated PAHs and heterocyclic compounds are more deleterious than the unsubstituted compounds (Yu, 2002; Rhodes et al., 2005; Turcotte et al., 2011; Lin et al., 2015). ~~Alkylated PACs are not as widely studied as unsubstituted PACs; however, given~~Considering the equivalent or increased potential for toxic effects, further studies~~y~~ ~~is~~ on alkylated PACs are warranted. It has also been observed that alkylated PAHs and DBTs are more abundant in petrogenic sources (Rhodes et al., 2005; Yang et al., 2011; Wickliffe et al., 2014) making it important to study PACs in oil sands regions.

Situated in Canada's boreal forest, the Athabasca oil sands region (AOSR) of northern Alberta is a concentrated area of industrial development with numerous facilities extracting and processing bitumen. This region makes up ~82% of the total bitumen in the oil sands deposits of northeastern Alberta, of which 20% (4,800 km^2) can be extracted by surface mining (Small et al., 2015). PAC emissions sources directly related to oil sands development include bitumen production facilities, mine face, mine fleet, and tailings ponds (Parajulee and Wania, 2014). Sources from non-industrial activities also contribute: wood burning, forest fires, and vehicular emissions have also been identified as sources of pervasive airborne PAHs (Hsu et al., 2015).

PAC emissions inventories for the AOSR are necessary for the modelling of PAC concentrations, deposition and subsequent assessments of ecosystem impacts. The Canadian National Pollutant Release Inventory (NPRI) contains speciated PAH emissions from point and fugitive sources in the AOSR; however, only the annual total facility emissions are required to be reported. There are two other emissions databases in the AOSR that are suitable for compiling a PAC emissions database. The Cumulative Environmental Management Association (CEMA) and Joint Canada-Alberta Oil Sands Monitoring (JOSM) emissions databases include spatially-resolved volatile organic compound (VOC) emissions data from additional source categories (e.g., tailings ponds, mine face, mine fleet, non-industrial), but not for PAC species. Thus, a comprehensive PAC emissions database needs to be developed that can provide speciated as well as spatially-resolved emissions data suitable for air quality modelling.

Quantifying the PAC emissions from the AOSR remains a significant challenge because of uncertainties in the emissions from oil sands production. A study estimated that PAH fluxes from tailings ponds were 4.6 times greater than the point source and fugitive emissions reported by the oil sands industry to the NPRI in 2012 (Galarneau et al., 2014a). Model simulations considering only direct air emissions underestimated phenanthrene, pyrene and benzo(*a*)pyrene concentrations in air, water, soil and foliage, whereas simulations including both direct air emissions and tailings pond emissions were more comparable to observations (Parajulee and Wania, 2014). Another source of airborne PAHs that has not been included in the emissions inventory is petroleum coke stockpiles in the mining areas, which can be resuspended by wind and deposited (Zhang et al., 2016). Analysis of wildlife samples near oil sands development indicate moose and wolves have been exposed to alkylated PAHs from petrogenic sources (Lundin et al., 2015). This study suggested that PACs are making their way through ecosystems in northern Alberta. However, the uncertainties in PAC emissions in this region need to be resolved in order to improve the understanding of how the emissions are impacting ecosystems.

In this study, two PAC emissions databases were developed. In the CEMA-derived emissions database, PAH emissions were estimated from PAH speciation profiles and CEMA emissions data which included VOC emissions from oil sands mining areas and non-industrial sources. In the JOSM-derived emissions database, several sources of data obtained from the JOSM program were used to estimate PAC emissions (i.e. PAH, alkylated PAH and DBT) including: VOC emissions from oil sands mining areas and non-industrial sources from the JOSM emissions database, tailings ponds emissions estimates (Galarneau et al., 2014a), and passive air concentrations (Schuster et al., 2015). The CALPUFF atmospheric dispersion model was then used to simulate PAC concentrations in the AOSR. Model simulations were conducted using the emissions from the CEMA-derived database in one scenario and the JOSM-derived database in another. The ~~modeled~~modelled concentrations of PAHs, alkylated PAHs and DBTs were compared with passive monitoring data to assess which emissions input can achieve better model-measurement agreement.

2 Methodology

2.1 Development of PAC emissions databases

2.1.1 CEMA and JOSM emissions databases

CEMA comprises aboriginal, government, non-governmental organizations, and industry stakeholders. CEMA’s role includes developing air quality management frameworks/plans for the Regional Municipality of Wood Buffalo (RMWB).

The implementation of these frameworks/plans is supported by ambient air quality and deposition modelling, which assesses the current and future environmental impacts of emissions from oil sands development and other local or regional sources in the RMWB including the AOSR (Vijayaraghavan et al., 2010). The models require a representative regional emissions database. The focus of the CEMA emissions database was to identify and quantify industrial and non-industrial emission sources in the AOSR. Industrial sources are comprised of stacks, mine fleet exhausts, fugitive plant, fugitive mine pit, fugitive tailings management, while non-industrial sources include community, highway (on-road), and recreational vehicle (off-road) sources (CEMA, 2011). This database is based on emissions data from 2009 to 2010.

The JOSM emissions database (ECCC and AEP, 2016) was developed by the Governments of Canada and Alberta. This database covers the oil sands areas and is based partially on existing emissions data from NPRI and CEMA. The JOSM database used in this study is based on the data available up to October 31, 2014 (ECCC, 2016). Neither the CEMA nor JOSM emissions database contain individual PAC species or total PACs. Instead, the databases report total VOCs, which includes PAHs and other hydrocarbons. Speciated PAH air emissions have been reported by the oil sands industries to the NPRI for point and fugitive sources (ECCC, 2017); however the actual source locations of the boilers, heaters, co-generation units, etc. belonging to each facility and stack dimensions and flow parameters are not required to be reported. Because these physical specifications are necessary to accurately model air pollution dispersion, the PAH emissions from the NPRI are not suitable for this study. Recently, PAHs disposed in tailings and waste rock were reported to the NPRI; however, the fluxes to air are unknown.

In this study, PAC emissions to air were estimated for a broad range of source categories using the VOC emissions in Table S1 of the Supplement. In the JOSM database, VOC emissions from tailings ponds, mine face and point sources have been scaled up from the CEMA database using the 2010 NPRI data. As shown in Table S1, VOC emissions from mine fleet, residential, commercial, non-industrial, and line sources (transportation) were relatively unchanged because the JOSM database adopted these emissions from the CEMA database. Oil sands mining emissions from the JOSM database are essentially the same as the CEMA database with partial updates for a few facilities using NPRI data and mining site spatial surrogates from satellite data. We assumed no changes to the point source VOC emissions because model sensitivity analysis indicated that point and line sources within the model domain have minimal impact on PAC concentrations in the oil sands mining areas (Sect. 3.~~2~~3). The major point sources are located south of the study area in the Southern Athabasca Oil Sands area, which is dominated by in-situ bitumen extraction. Geospatial data from the databases indicate that oil sands mining areas have increased from the CEMA to the JOSM database. The surface area of tailings ponds grew from 104.7 km^2 in the CEMA database to 182.6 km^2 in the JOSM database (Fig. S1 of the Supplement), while mine face areas increased from 35.1 km^2 to 170.1 km^2.

2.1.2 Estimation of PAC emissions and speciation methodology

CEMA-derived and JOSM-derived emissions for PACs were estimated for the following source categories: 1) tailings ponds; 2) mine face; 3) mine fleet; and 4) other sources including point sources, transportation, residential, and commercial. Different approaches were taken to estimate the PAH emissions from the various source categories; the details are described in Sect. S1 of the Supplement. For 1) tailings ponds, the PAH emission speciation was based on the study by Galarneau et al. (2014a). This study reported emissions of 1,069 kg yr^{-1} from tailings ponds for 13 PAH species during the JOSM field campaign (2010-2012). The annual emissions were distributed between the individual tailings ponds using the area of the tailings ponds. For 2) mine face PAH emissions, an assumption was made that the emission flux of PAH species volatilized from the mine face would be lower than that of tailings ponds based on the ratio of the VOC emissions from these sources. There were no direct emissions measurements available from a mine face in the oil sands area at the time of this study. For 3) mine fleet, PAHs were speciated by mass fraction of total VOC emissions from mine fleet based on the CEMA study (Vijayaraghavan et al., 2010). CEMA's mine fleet PAH speciation profiles were developed using the USEPA SPECIATE database (USEPA, 2017). For 4) other emissions, speciation of both point and non-point source emissions was based on VOC and $PM_{2.5}$ emissions and speciation profiles in the CEMA study by Vijayaraghavan et al. (2010). Note that the majority of CEMA speciation profiles were based on a series of environmental impact assessment studies in the oil sands area (Vijayaraghavan et al., 2010). For those point and non-point sources that were not available in the CEMA database, PAH species were estimated using SPECIATE (USEPA, 2017), which has a repository of organic and PM speciation profiles for various air pollution sources (Simon et al., 2010). The profiles can be used to create speciated emissions inventories for ozone modelling (e.g. NO, NO_2, and explicit VOC species) and estimate hazardous and toxic air pollutant emissions from total PM and organic primary emissions. For alkylated PAHs and DBTs, emissions from mine fleet and transportation were estimated using SPECIATE, while an approach using the ratio of total PAH to alkylated PAH or DBT from passive sampling data was used to calculate tailings pond emissions. Based on the expansion of the tailings ponds and mine face surface areas from the CEMA to JOSM databases which in turn led to higher VOC emissions from these sources (Table S1 and ~~sect~~Sect. S1 of the Supplement), most of the PAH emission increases are attributed to tailings ponds and mine face sources.

~~The estimated emissions of total PAHs, alkylated PAHs, and DBTs from the various source categories are shown in Table 1. It was found that there were still gaps in the existing emissions database, and speciation profiles were largely missing particularly for alkylated PAHs and DBTs. In this paper, the focus is on PAHs; however, alkylated PAHs and DBTs were still modelled despite the limited knowledge of emissions profiles.~~

2.2 CALPUFF model

The ~~USEPA~~ CALPUFF model was run using the CEMA-derived or JOSM-derived emissions database for PACs, and the PAC concentrations downwind were predicted. CALPUFF is an advanced, integrated Lagrangian puff modelling system for the simulation of atmospheric pollution dispersion adopted by the USEPA in its Guideline on Air Quality Models and accepted by Alberta Environment and Parks and the Alberta Energy Regulator. CALPUFF takes three-dimensionally varying wind, temperature and turbulence fields from the CALMET model. ~~which is a stand-alone meteorological data processor. In this study, CALMET harmonizes Weather Research and Forecasting (WRF) generated three-dimensional data and local observed data together. The WRF Model is a next-generation mesoscale numerical weather prediction system designed for both atmospheric research and operational forecasting needs (Skamarock et al., 2008).~~ The 3-D winds and temperature fields from CALMET are reconstructed using meteorological measurements, orography and land use data. Besides wind and temperature fields, CALMET determines the 2-D fields of micrometeorological variables needed to carry out dispersion simulations (mixing height, Monin Obukhov length, friction velocity, convective velocity, etc.). A two-step approach is typically used to compute the wind fields in CALMET. In the first step, an initial guess wind field is adjusted for kinematic effects of terrain, slope flows, and terrain blocking effects. The second step applies an objective analysis procedure to introduce observational data into the first step to produce the final wind fields. In this study, CALMET used the Weather Research and Forecasting (WRF) model due to its capability of simulating regional flows and certain aspects of local meteorological conditions such as complex terrain. It replaces the two-step approach given the higher spatial resolution of the WRF output compared to observational data. The output of the CALMET model is directly interfaced with the CALPUFF dispersion model for further air quality modelling.

CALPUFF was set up and modelled following the Alberta Air Quality Model Guideline (AEP, 2013). ~~-~~The model was run from October 2010 to the end of 2012. ~~For this study, the CALPUFF~~The model simulated the dispersion and transport of PACs~~ and estimated the ambient air concentrations. H~~; however, the dry and wet deposition schemes were not activated in the model~~,~~ and the chemical processes were limited for modelled PAC species. The model predicted the concentrations of 16 USEPA priority PAHs for the CEMA-derived and JOSM-derived emissions scenarios: naphthalene (NAPH), acenaphthylene (ACY), acenaphthene (ACE), fluorene (FLR), phenanthrene (PHEN), anthracene (ANTH), fluoranthene (FLRT), pyrene (PYR), benz[a]anthracene (BaA), coeluting chrysene and triphenylene (CHRYþTRIP), benzo[b]fluoranthene (BbF), benzo[k]fluoranthene (BkF), benzo[a]pyrene (BaP), indeno[1,2,3-cd]pyrene (I123cdP), dibenz[a,h]anthracene (dBahA) and benzo[ghi]perylene (BghiP).~~, as well as total alkylated PAHs and DBTs.~~ Note that retene (methyl isopropyl phenanthrene) was categorized as part of total alkylated PAHs. Total alkylated PAHs and DBT concentrations were modelled for the JOSM-derived emissions scenario only, since the monitoring of these additional compounds is part of monitoring activities under the JOSM program. ~~Note that retene (methyl isopropyl phenanthrene) was categorized as part of total alkylated PAHs.~~

~~CALPUFF modelling was applied to both discrete receptors (i.e. sensitive receptors) and gridded receptors (i.e. CALPUFF modelling grids).~~ The CALPUFF modelling domain covers a large area bounded by the following coordinates, SW: 54.599, -

114.000, SE: 54.595, -107.807, NW: 59.766, -114.450, NE: 59.760, -107.328. The model domain is larger than the study area, which is focused on the oil sands mining areas (Fig. S2). ~~It covers all possible sources including traffic and transportation along the road network, industrial areas, residential/commercial sources, and the northern part of Edmonton (urban area).~~ Emissions outside the model domain are not accounted for in the model. Further details regarding the CALPUFF model settings and options are provided in Sect. S2 of the Supplement.

2.3 Model evaluation against passive monitoring data

Model-predicted PAC concentrations were compared with measurements from a 17-site passive air sampling network (Fig. S1; Harner et al., 2013; Schuster et al., 2015). The model evaluation domain focused on a specific area (Fig. S1a; SW: 56.272, -112.260, SE: 56.278, -110.452, NW: 57.880, -112.315, NE: 57.885,-110.428). Figure S1b illustrates the locations of the passive air samplers in the AOSR. The PAC data was collected from 172 samples at 17 sites between November 2010 and June 2012. There are 8 local sites (L) which are accessible by road and near oil sands operations and 9 remote sites (R). PAH concentrations were relatively constant throughout most of the sampling period, except for elevated concentrations observed from April to July 2011 which were attributed to forest fires events (Schuster et al., 2015). The forest fire events were identified based on high retene concentrations and retene/(retene+chrysene) ratio approaching one (Schuster et al., 2015). ~~Biomass, fossil fuel, and petrogenic combustion can also be distinguished based on fluoranthene/(fluoranthene+pyrene) ratio (Lundin et al., 2015).~~ Data collected during the forest fire period were excluded from the model~~ling~~ evaluation because PAH emissions from forest fires were not inputted into the model. Additionally, site L14 showed extremely high PAH concentrations during the summer months, which was also excluded from model evaluation. The higher summertime concentrations at site L14 was likely due to revolatilization of PAHs from nearby Gregoire Lake (Hsu et al., 2015). Furthermore, due to the high volatility of NAPH leading to sampling biases (Harner et al., 2013) and the high NAPH concentrations (one to two orders of magnitude higher than all other PACs), we took NAPH out from the total PAH group and treated it separately to avoid masking the other PAC species.

3 Results and Discussion

3.1 PAC emissions estimates

Over the model domain, the total unsubstituted PAH emissions (2009-2014) are estimated to be 56 to 58 tonnes yr^{-1} based on emissions from tailings ponds, mine face, mine fleet, residential, commercial, local traffic, airport, point, and transportation sources (Table 1). A map of the spatial distribution of the emissions is shown in Fig. S3 of the Supplement. Point sources accounted for most of the total unsubstituted PAH emissions (75-77%). The major difference in the total unsubstituted PAH emissions between the CEMA-derived and JOSM-derived emissions databases is the higher evaporative PAH emissions from tailings ponds and mine face in the JOSM-derived emissions database. Alkylated PAH and DBT emissions (2011-

2014) are estimated to be 17 tonnes yr^{-1} and 0.26 tonnes yr^{-1} respectively; however, they consisted of fewer emission sources (tailings ponds, mine fleet and transportation sources) due to a lack of PAC speciation data to estimate these emissions. Nevertheless, the PAC emissions estimates may still be underestimated from oil sands sources, such as tailings ponds and fugitive dust. Recent studies suggest that flux chamber measurements of tailings pond emissions underestimate organic compound emission fluxes (Tran et al., 2018). Windblown petcoke dust observed recently over surface mining areas in the AOSR (Zhang et al., 2016) also have not been accounted for in the PAC emissions databases. In addition to gaps in the existing emissions databases, speciation profiles were largely missing particularly for alkylated PAHs and DBTs. In this paper, the focus is on unsubstituted PAHs; however, alkylated PAHs and DBTs were still modelled despite the limited knowledge of the emissions profiles.

3.~~1~~ 2 Total PAH concentrations

~~In this study, total PAHs included all PAHs measured during the JOSM program in 2010-2012 except NAPH as mentioned above.~~ Figure 1 shows a comparison of the average total PAH concentrations (excluding NAPH) between the CALPUFF model and passive measurements at local and remote sites. Site L14 and data that had been impacted by forest fires were excluded in Figure 1 as explained above. The modelled results included two emissions input scenarios: CEMA-derived and JOSM-derived PAC emissions. Note that the CALPUFF air quality modelling runs used the same meteorological data input from CALMET and the same CALPUFF model settings. The only difference was the use of different PAC emissions data.

Overall, it can be seen that the model performed much better at local sites than at remote sites as shown in Figures 1a and 1b, respectively. CALPUFF was capable of reproducing the passive measurements at the local sites particularly at L04, L06 and L13, but underestimated PAHs considerably at remote sites except at R05. Figure 1 also suggests that model-JOSM case performed better than the model-CEMA case at most of the sites, except R05. These results suggest that the improvements to the JOSM-derived emissions database led to better agreement between model and observations than the CEMA-derived emissions database.

In terms of the model performance, the model percentage errors at local sites were much smaller than remote sites: 17% vs. 66% with JOSM-derived emissions, and 30% vs. 67% with CEMA-derived emissions (Table S2). While model-JOSM performed better than model-CEMA at the local sites, little improvement was found at the remote sites. Modelled concentrations produced using either the CEMA-derived or JOSM-derived emissions data were underestimated by a factor of 3. This suggests that the changes in oil sands emissions from CEMA-derived to JOSM-derived database had essentially an insignificant impact on modelling results in the remote area. Model underestimation of PAH concentrations at most of the remote sites could be due in part to small forest fires in the remote area. Based on the fire radiative power (FRP) data from MODIS (NASA, 2017), 14 of the 17 passive sampling sites were strongly impacted by forest fires from April to July 2011 (Fig. ~~S3a~~S4a). Thus, the passive measurements collected during this period were omitted from the model evaluation. During other times of the year in 2011 and 2012, most of the sites were unaffected by large forest fires although the R01, R08 and R09 remote sites may have been affected by small fires nearby (Fig. ~~S3b~~S4b).

Besides forest fires, elevated regional background levels of PAHs in air from long-range transport of emissions and re-emissions to air of previously deposited PAHs that are not accounted for in the model could explain the underestimated concentrations at remote sites. While the model did not include long-range emissions transport, the lack of deposition loss of PAHs in the model may partially compensate for the missing background emissions in the model. Presenting the model results without deposition loss also allowed us to assess whether the emissions estimates were reasonable. This is because the modelled concentrations from simulating emissions, transport and dispersion processes without deposition loss are already lower than measurements, which suggest that the emissions input are conservative or underestimated. One of the impacts of turning off deposition modelling is that the modelled air concentrations are higher compared to those with deposition modelling turned on. If deposition had been considered~~ in the model~~, the ~~modeled~~modelled concentrations would be even lower than the current predictions. However, in this model scenario we cannot be certain if this is caused by too low emissions input or too high deposition rates, knowing that large uncertainties exist in modelling dry and wet deposition processes. For example, there are large uncertainties in the PAC dry deposition velocities (Zhang et al., 2015a), PAC scavenging ratios for snow and rain scavenging of gas-phase and particulate-phase PACs (Zhang et al., 2015b), and scavenging coefficients of aerosols by snow and rain scavenging processes (Zhang et al., 2013; Wang et al., 2014).

3.~~2~~ 3 Spatial distribution of PAH concentrations

Figure 2 illustrates the spatial distribution of the model-predicted average PAH concentrations using CEMA-derived (2a) and JOSM-derived (2b) emissions, overlaid with passive measurements from November 2010 to June 2012. The contours in Figure 2 were produced from the model outputs; the coloured dots represent PAH measurements at the 17 passive sampling sites~~; the colour legend and the scale represent PAH concentrations in ng m^{-3}. If the contour colour matches the dot colour, the model is able to reproduce the measured data.~~.

A comparison of Figures 2a and 2b shows that the model-JOSM (2b) reproduced the elevated PAH concentrations over major mining areas, such as areas south of Fort McKay, Mildred Lake settling basin, tailings ponds owned by Suncor Energy, and tailings ponds located north of Fort McKay owned by Syncrude Canada Ltd. Model-JOSM was the better model at most of the local sites (contour colours closely match the dot colours). Point sources and transportation emissions had minor impacts on modelled PAH concentrations according to the model sensitivity analysis (Fig. ~~S4~~S5). Although PAH emissions from point sources were greater than the emissions from other source categories (Table 1), this did not result in higher ground level concentrations near the point sources. For point sources, other factors such as stack heights, exit temperatures and exit velocities are also important to plume rise and dispersion, which can lead to lower ground level concentrations compared to those impacted by similar emissions from area sources such as tailings ponds. The impact at ground level from point sources is based on a combination of factors, not only on the emission rates.

CALPUFF significantly underestimated the PAH concentrations in remote areas regardless of the emissions data input. High PAH concentrations at remote sites are unlikely to be subject to industrial emissions. Thus, there are likely other sources of PAHs, such as small forest fires that contributed to the elevated PAH concentrations and re-volatilization of previously deposited PAHs, which were not considered in the model. The underestimation by the model could also be due to the underestimation of VOC emissions in the AOSR (Li et al., 2017), since PAC emissions from mine fleet, point sources, transportation, residential and commercial sources were derived from VOC emissions and speciation profiles.

The model-JOSM (Fig. 2b) output also suggests that high PAH concentrations were not necessarily located at local sites. For example, sites L01, L04 and L05 are located east of Syncrude Canada's Mildred Lake tailings facilities, while the area with highest PAH concentrations were found northeast of the monitoring sites. A similar effect was also observed at local sites west of the Suncor Energy tailings ponds.

3.~~3~~ 4 PAH speciation analysis

Figures 3a and b illustrate the ratios of speciated PAH modelled-to-measured concentrations for all of the valid data pairs available for the model evaluations, with both CEMA-derived and JOSM-derived emissions. The ratios for local and remote sites are shown in Fig. 3a and b, respectively. CEMA and JOSM modelled concentrations and measured concentrations averaged from all sites are illustrated in Fig. 3c and d.

For local sites, there were 5 PAH species (ANTH, BaA, CHRYþTRIP, BbF, and BghiP) from model-JOSM (orange dots) for which the model agreed with measured concentrations within a factor of 2. The average modelled-to-measured concentration ratios for these 5 species were 1.6, 0.9, 0.5, 0.5 and 1.1, respectively. Only 3 PAH species (ANTH, BaA and BghiP) from model-CEMA (blue dots) yielded average modelled-to-measured concentration ratios that were close to the ideal value of unity (1.7, 0.7 and 1.5, respectively). Similar patterns were found at remote sites. Comparison of the modelled speciated PAH concentrations from all the sites (Fig. 3c,d) between the CEMA-derived and JOSM-derived emissions scenarios show there were minor differences in most of the PAH species, including NAPH, ACY, ACE, FLR, ANTH, FLRT, BkF, I123cdP, and dBahA. The model output using the JOSM-derived emissions predicted higher concentrations that were closer to the observed concentrations than of the CEMA-derived emissions for PHEN, BaA, CHRYþTRIP, BbF, and BaP. For the species ACY, FLRT and PYR, both emissions scenarios overestimated the observed concentrations. The dominant PAH species from passive measurements were NAPH, PHEN, and FLR. In another study using high-volume sampling methods to measure PAHs from the AOSR, PHEN, NAPH, and ANTH were the most abundant species (Wnorowski, 2017). However in our model simulations, the dominant PAH species were NAPH, PYR, and PHEN for the JOSM-derived emissions scenario and NAPH, PYR, and ACY for the CEMA-derived emissions scenario. The discrepancies in the dominant PAH species between the model and measurements suggest uncertainties in the PAH speciation profiles for oil sands sources.

3.~~4~~ 5 Total alkylated PAH and DBT concentrations

The modelled concentrations of total alkylated PAH and DBT from the JOSM-derived emissions database were underpredicted compared to the measurements from the passive sampling network (Fig. 4). This could be due to (1) a lack of emissions estimates from other oil sands sources, such as mine face and facility fugitive emissions (e.g. Zhang et al., 2016), since alkylated PAH and DBT emissions were only estimated from mine fleet, line sources, and tailings ponds; and (2) uncertainties with using monitored concentration ratios (*R*) between PAHs and alkylated PAHs/DBTs to back-calculate alkylated PAH and DBT emissions (~~sect~~Sect. 1.5 in the ~~SI~~Supplement). In this study, we assumed a constant average ratio for PAH/alkylated PAH and PAH/DBT; however, this ratio could change depending on where the monitoring sites are located because of other emission sources and the decline in PAC deposition with distance from major oil sands development areas (Manzano et al., 2016).

4 Conclusions

The JOSM-derived emissions database improved CALPUFF model predictions of total PAH concentrations against passive monitoring data at local sites compared to using the CEMA-derived emissions database. The model significantly underestimated PAH concentrations at most of the remote locations. Although the data impacted by major forest fire events were excluded from model evaluation, it is possible that unreported small forest fires, re-emissions of previously deposited PAHs, and long-range transport contributed to the elevated PAH concentrations at remote sites. For alkylated PAHs and DBTs, the model underestimated the concentrations at all of the sites.

One of the emissions gaps identified in this study is a lack of emissions data on alkylated PAHs and DBTs. Uncertainties in the methodology for estimating PAC emissions and speciation profiles of PACs from different oil sands emission sources are potential reasons for the discrepancies between model results and observations. These issues need to be resolved to better model the PAC concentrations and deposition in this region. Using a dispersion model, such as CALPUFF with detailed 3-D meteorological fields generated by WRF/CALMET, to drive air dispersion from oil sands emissions sources can provide a better understanding of PAC spatial distribution patterns. Model results can identify potential “hot~~-~~spots” with the highest concentrations, which can be used to guide monitoring network design. For instance, modelling results from this study suggest the current PAH monitoring sites are not located within the highest modelled concentration areas which are adjacent to major tailings ponds and mines. The addition of an air–surface exchange parameterization should be evaluated as a potential response to the seasonally varying prediction capabilities of the model for the most volatile compounds.

Data Availability

The data from this study are accessible from the links provided in the references.

Competing Interests

The authors declare that they have no conflict of interest.

Acknowledgements

This work was supported by the Climate Change and Air Pollutants program of Environment and Climate Change Canada (ECCC) and by the Province of Alberta through the Oil Sands Monitoring program. ~~We acknowledge funding support from the Joint Canada-Alberta Implementation Plan for Oil Sands Monitoring (JOSM) program,~~ We also acknowledge Alberta Environment and Parks (AEP) for providing some of the oil sands data used in the study~~,~~ and the use of data and imagery from LANCE FIRMS operated by the NASA/GSFC/Earth Science Data and Information System (ESDIS) with funding provided by NASA/HQ. The authors thank Stewart Cober, Elisabeth Galarneau, Jasmin Schuster, and Andrzej Wnorowski from ECCC, Canada's Oil Sands Innovation Alliance (COSIA) and AEP for comments that helped improve the paper; ~~and~~ Amy Hou from ECCC for producing the emissions map (Fig. S3); and Junhua Zhang from ECCC for advice on the JOSM emissions database.

References

Alberta Environment and Parks (AEP): Air Quality Model Guideline (AQMG), available at https://extranet.gov.ab.ca/env/infocentre/info/library/8908.pdf, 2013.

Agency for Toxic Substances and Disease Registry (ATSDR): Case Studies in Environmental Medicine, Toxicity of Polycyclic Aromatic Hydrocarbons, pp. 68, 2009.

~~Baek, S. O., Field, R. A., Goldstone, M. E., Kirk, P. W., Lester, J. N., and Perry, R.: A review of atmospheric polycyclic aromatic hydrocarbons: sources, fate and behavior, Water Air Soil Pollut., 60(3-4), 279-300, 1991.~~

~~Boström, C. E., P. Gerde, A. Hanberg, B. Jernström, C. Johansson, T. Kyrklund, A. Rannug, M. Törnqvist, K. Victorin, and R. Westerholm: Cancer risk assessment, indicators, and guidelines for polycyclic aromatic hydrocarbons in the ambient air, Environ. Health Perspect., 110, suppl. 3, 451–488, 2002.~~

CCME (Canadian Council of Ministers of the Environment): Canadian Soil Quality Guidelines for Carcinogenic and Other Polycyclic Aromatic Hydrocarbons (Environmental and Human Health Effects), Scientific Criteria Document (revised), pp. 216, 2010.

Cumulative Environmental Management Association (CEMA): Lower Athabasca Region Source and Emission Inventory. Fort McMurray, Alberta. Available at: http://library.cemaonline.ca/ckan/dataset/2011-0038/resource/fba8a3b0-72df-45ed-bf12-8ca254fdd5b1, 2011.

Environment and Climate Change Canada (ECCC): Source Emissions, Oil Sands Region, Emissions-package, available at: http://donnees.ec.gc.ca/data/air/monitor/source-emissions-monitoring-oil-sands-region/source-emissions-oil-sands-region/emissions-package/?lang=en, 2016.

Environment and Climate Change Canada (ECCC) and Alberta Environment and Parks (AEP), 2016: Joint Oil Sands Monitoring Program Emissions Inventory Compilation Report, June 2016, available at: http://aep.alberta.ca/air/reports-data/air-emissions-inventory.aspx, 2016.

ECCC: National Pollutant Release Inventory – Bulk Data, available at: http://open.canada.ca/data/en/dataset/40e01423-7728-429c-ac9d-2954385ccdfb, 2017.

Galarneau, E., Hollebone, B. P., Yang, Z., and Schuster, J.: Preliminary measurement-based estimates of PAH emissions from oil sands tailings ponds, Atmos. Environ., 97, 332-335, 2014a.

Galarneau, E., Makar, P. A., Zheng, Q., Narayan, J., Zhang, J., Moran, M. D., Bari, M. A., Pathela, S., Chen, A., and Chlumsky, R.: PAH concentrations simulated with the AURAMS-PAH chemical transport model over Canada and the USA, Atmos. Chem. Phys., 14, 4065-4077, 2014b.

Giesy, J. P., Anderson, J. C., and Wiseman, S. B.: Alberta oil sands development, Proc. Natl. Acad. Sci., 107(3), 951-952, 2010.

Gosselin, P., Hrudey, S. E., Naeth, M. A., Plourde, A., Therrien, R., Van Der Kraak, G., and Xu, Z.: The Royal Society of Canada Expert Panel: Environmental and health impacts of Canada's oil sands industry. December 2010, The Royal Society of Canada Academies of Arts, Humanities and Sciences of Canada, Available at: https://www.ceaa-acee.gc.ca/050/documents_staticpost/59540/82080/Appendix_E_-_Part_09.pdf, 2010.

Harner, T., Su, K., Genualdi, S., Karpowicz, J., Ahrens, L., Mihele, C., Schuster, J., Charland, J. -P. and Narayan, J.: Calibration and application of PUF disk passive air samplers for tracking polycyclic aromatic compounds (PACs), Atmos. Environ., 75, 123-128, 2013.

Hsu, Y. M., Harner, T., Li, H., and Fellin, P.: PAH measurements in air in the Athabasca oil sands region, Environ. Sci. Technol., *49*(9), 5584-5592, 2015.

Jariyasopit, N., Harner, T., Wu, D., Williams, A., Halappanavar, S., Su, K.: Mapping indicators of toxicity for polycyclic aromatic compounds in the atmosphere of the Athabasca oil sands region, *Environ. Sci. Technol.*, *50*, 11282-11291, 2016.

Jautzy, J., Ahad, J. M., Gobeil, C., and Savard, M. M.: Century-long source apportionment of PAHs in Athabasca oil sands region lakes using diagnostic ratios and compound-specific carbon isotope signatures, Environ. Sci. Technol., 47(12), 6155-6163, 2013.

~~Keyte, I. J., Harrison, R. M., and Lammel, G.: Chemical reactivity and long-range transport potential of polycyclic aromatic hydrocarbons–a review, Chem. Soc. Rev., 42(24), 9333-9391, 2013.~~

Kim, K. H., Jahan, S. A., Kabir, E., and Brown, R. J.: A review of airborne polycyclic aromatic hydrocarbons (PAHs) and their human health effects, Environ. Int., 60, 71-80, 2013.

Li, S. M., Leithead, A., Moussa, S. G., Liggio, J., Moran, M. D., Wang, D., Hayden, K., Darlington, A., Gordon, M., Staebler, R., Makar, P. A., Stroud, C. A., McLaren, R., Liu, P. S. K., O'Brien, J., Mittermeier, R. L., Zhang, J., Marson, G., Cober, S. G., Wolde, M., and Wentzell, J. J. B.: Differences between measured and reported volatile organic compound emissions from oil sands facilities in Alberta, Canada, Proc. Natl. Acad. Sci., 114(19), E3756-E3765, 2017.

Lin, H., Morandi, G. D., Brown, R. S., Snieckus, V., Rantanen, T., Jørgensen, K. B., and Hodson, P. V.: Quantitative structure–activity relationships for chronic toxicity of alkyl-chrysenes and alkyl-benz[a]anthracenes to Japanese medaka embryos (Oryzias latipes), Aquatic Toxicol., 159, 109-118, 2015.

Lundin, J. I., Riffell, J. A., and Wasser, S. K.: Polycyclic aromatic hydrocarbons in caribou, moose, and wolf scat samples from three areas of the Alberta oil sands, Environ. Pollut., 206, 527-534, 2015.

Manzano, C. A., Marvin, C. H., Muir, D. C., Harner, T., Martin, J. W., and Zhang, Y.: Heterocyclic aromatics in petroleum coke, snow, lake sediments and air samples from the Athabasca oil sands region, Environ. Sci. Technol., 51, 5445-5453, 2017.

Manzano, C.A., Muir, D., Kirk, J., Teixeira, C., Siu, M., Wang, X., Charland, J.P., Schindler, D. and Kelly, E.: Temporal variation in the deposition of polycyclic aromatic compounds in snow in the Athabasca Oil Sands area of Alberta, Environ. Monit. Assess., 188(9), 542, 2016.

NASA: MODIS Collection 6 NRT Hotspot / Active Fire Detections MCD14DL. DOI: 10.5067/FIRMS/MODIS/MCD14DL.NRT.006, 2017.

~~Neff, J. M., Stout, S. A., and Gunster, D. G.: Ecological risk assessment of polycyclic aromatic hydrocarbons in sediments: identifying sources and ecological hazard, Integr. Environ. Assess. Manag., 1(1), 22-33, 2005.~~

Parajulee, A. and Wania, F.: Evaluating officially reported polycyclic aromatic hydrocarbon emissions in the Athabasca oil sands region with a multimedia fate model, Proc. Natl. Acad. Sci., 111(9), 3344-3349, 2014.

Rhodes, S., Farwell, A., Hewitt, L. M., MacKinnon, M., and Dixon, D. G.: The effects of dimethylated and alkylated polycyclic aromatic hydrocarbons on the embryonic development of the Japanese medaka, Ecotoxicol. Environ. Safety, 60(3), 247-258, 2005.

Schuster, J. K., Harner, T., Su, K., Mihele, C., and Eng, A.: First Results from the Oil Sands Passive Air Monitoring Network for Polycyclic Aromatic Compounds, Environ. Sci. Technol., 49, 2991–2998, 2015.

Simon, H., Beck, L., Bhave, P. V., Divita, F., Hsu, Y., Luecken, D., Mobley, J. D., Pouliot, G. A., Reff, A., Sarwar, G. and Strum, M.: The development and uses of EPA's SPECIATE database, Atmos. Pollut. Res., 1(4), 196-206, 2010.

~~Skamarock, W. C., Klemp, J. B., Dudhia, J., Gill, D. O., Barker, D. M., Duda, M. G., Huang, X.-Y., Wang, W., and Powers, J. G.: A Description of the Advanced Research WRF Version 3, NCAR Tech. Note NCAR/TN-475+STR, pp. 113, doi:10.5065/D68S4MVH, 2008.~~

Small, C. C., Cho, S., Hashisho, Z., and Ulrich, A. C.: Emissions from oil sands tailings ponds: Review of tailings pond parameters and emission estimates, J. Pet. Sci. Eng., 127, 490-501, 2015.

Timoney, K. P. and Lee, P.: Polycyclic aromatic hydrocarbons increase in Athabasca River Delta sediment: Temporal trends and environmental correlates, Environ. Sci. Technol., 45(10), 4278-4284, 2011.

Tran, H. N. Q., Lyman, S. N., Mansfield, M. L., O'Neil, T., Bowers, R. L., Smith, A. P. and Keslar, C.: Emissions of Organic Compounds from Produced Water Ponds II: Evaluation of flux-chamber measurements with inverse-modeling techniques, J. Air Waste Manag. Assoc., DOI: 10.1080/10962247.2018.1426654, 2018.

Turcotte, D., Akhtar, P., Bowerman, M., Kiparissis, Y., Brown, R. S., and Hodson, P. V.: Measuring the toxicity of alkyl-phenanthrenes to early life stages of medaka (Oryzias latipes) using partition-controlled delivery, *Environ. Toxicol. Chem.*, *30*(2), 487-495, 2011.

USEPA: SPECIATE 4.5, available at: https://cfpub.epa.gov/speciate/, 2017.

Vijayaraghavan, K., Nopmongcol, U., Grant, J., Morris, R., Pollock, T., Davies, M., Person, R.: Protocol for updating and preparing a modelling emission inventory. Cumulative Environmental Management Association, Fort McMurray, Alberta, Canada, available at: http://library.cemaonline.ca/ckan/dataset/2010-0031/resource/8f449c5d-3129-4d6f-a530-46ec33a46208, 2010.

Wang, X., Zhang, L., and Moran, M. D.: Development of a new semi-empirical parameterization for below-cloud scavenging of size-resolved aerosol particles by both rain and snow, Geosci. Model Dev., 7, 799-819, 2014.

Wickliffe, J., Overton, E., Frickel, S., Howard, J., Wilson, M., Simon, B., Echsner, S., Nguyen, D., Gauthe, D., Blake, D. and Miller, C., Elferink, C., Ansari, S., Fernando, H., Trapido, E., and Kane, A.: Evaluation of polycyclic aromatic hydrocarbons using analytical methods, toxicology, and risk assessment research: seafood safety after a petroleum spill as an example, Environ. Health Persp., 122(1), 6-9, 2014.

Wnorowski, A.: Characterization of the ambient air content of parent polycyclic aromatic hydrocarbons in the Fort McKay region (Canada), Chemosphere, *174*, 371-379, 2017.

Yang, C., Wang, Z., Yang, Z., Hollebone, B., Brown, C. E., Landriault, M., and Fieldhouse, B.: Chemical fingerprints of Alberta oil sands and related petroleum products, Environ. Forensics, 12(2), 173-188, 2011.

Yu, H.: Environmental carcinogenic polycyclic aromatic hydrocarbons: photochemistry and phototoxicity, J. Environ. Sci. Health Part C, 20(2), 149-183, 2002.

Zhang, L., Wang, X., Moran, M. D., and Feng, J.: Review and uncertainty assessment of size-resolved scavenging coefficient formulations for below-cloud snow scavenging of atmospheric aerosols, Atmos. Chem. Phys., 13, 10005-10025, 2013.

Zhang, L., Cheng, I., Muir, D., and Charland, J.-P.: Scavenging ratios of polycyclic aromatic compounds in rain and snow in the Athabasca oil sands region, Atmos. Chem. Phys., 15, 1421-1434, 2015b.

Zhang, L., Cheng, I., Wu, Z., Harner, T., Schuster, J., Charland, J. P., Muir, D., and Parnis, J.M.: Dry deposition of PACs to various land covers in the Athabasca Oil Sands Region, J. Adv. Model. Earth Sy., 7, 1339-1350, 2015a.

Zhang, Y., Shotyk, W., Zaccone, C., Noernberg, T., Pelletier, R., Bicalho, B., Froese, D. G., Davies, L. and Martin, J. W.~~, 2016~~: Airborne petcoke dust is a major source of polycyclic aromatic hydrocarbons in the Athabasca Oil Sands Region, Environ. Sci. Technol., 50(4), 1711-1720, 2016.

Table 1. Estimated PAH, alkylated PAH, and DBT emissions (kg yr^{-1}) over the model domain

	PAH		Alkylated PAH	DBT
	CEMA-derived emissions	JOSM-derived emissions	JOSM-derived emissions	JOSM-derived emissions
Tailings pond	417	1,069	2,442	255
Mine face	24	600	na	na
Mine fleet	9,573	9,698	7,596	0
Residential and commercial	58	58	na	na
Non-industry (local traffic and airport)	1,628	1628	na	na
Point sources	43,299	43,299	na	na
Line sources	1,401	1,401	7,200	3

na: not available

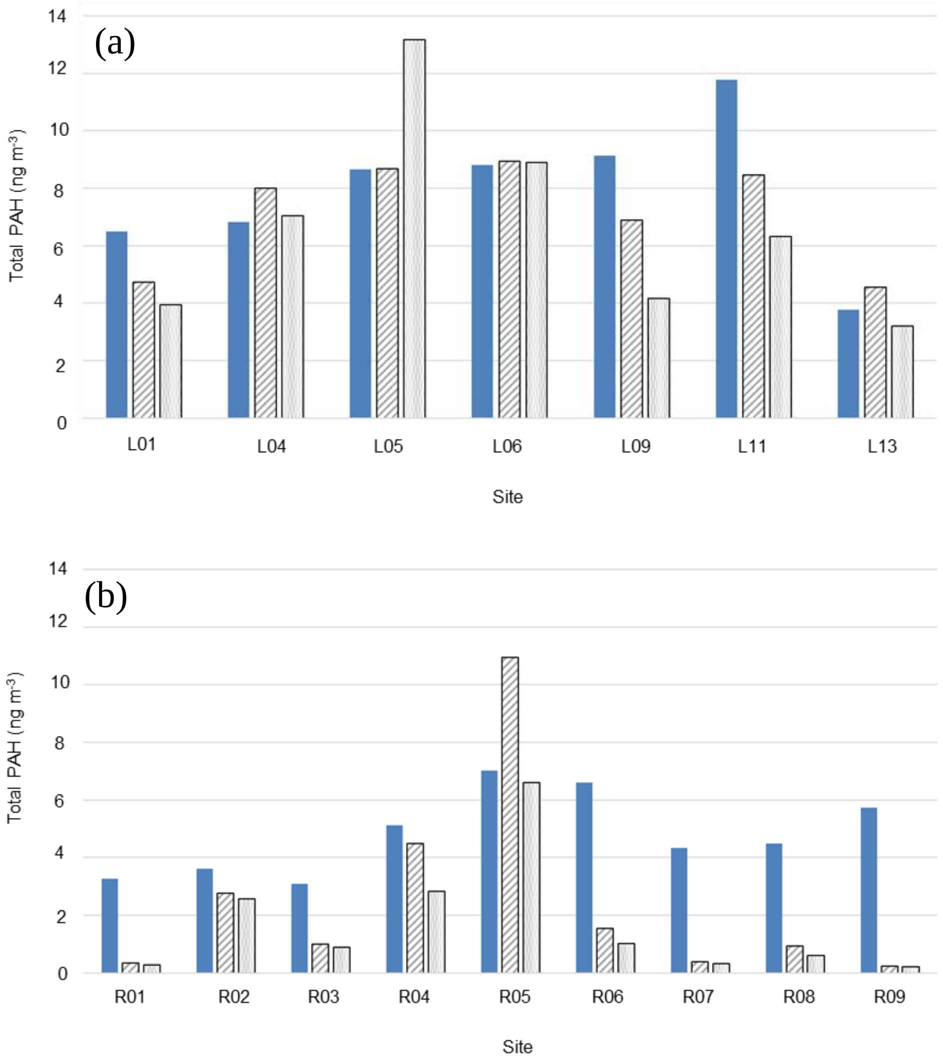

Figure 1: Average total PAH concentrations (excluding NAPH) from November 2010 to June 2012 at local (a) and remote sites (b): passive measurements (blue), modelled-JOSM case (striped) and modelled-CEMA case (grey).

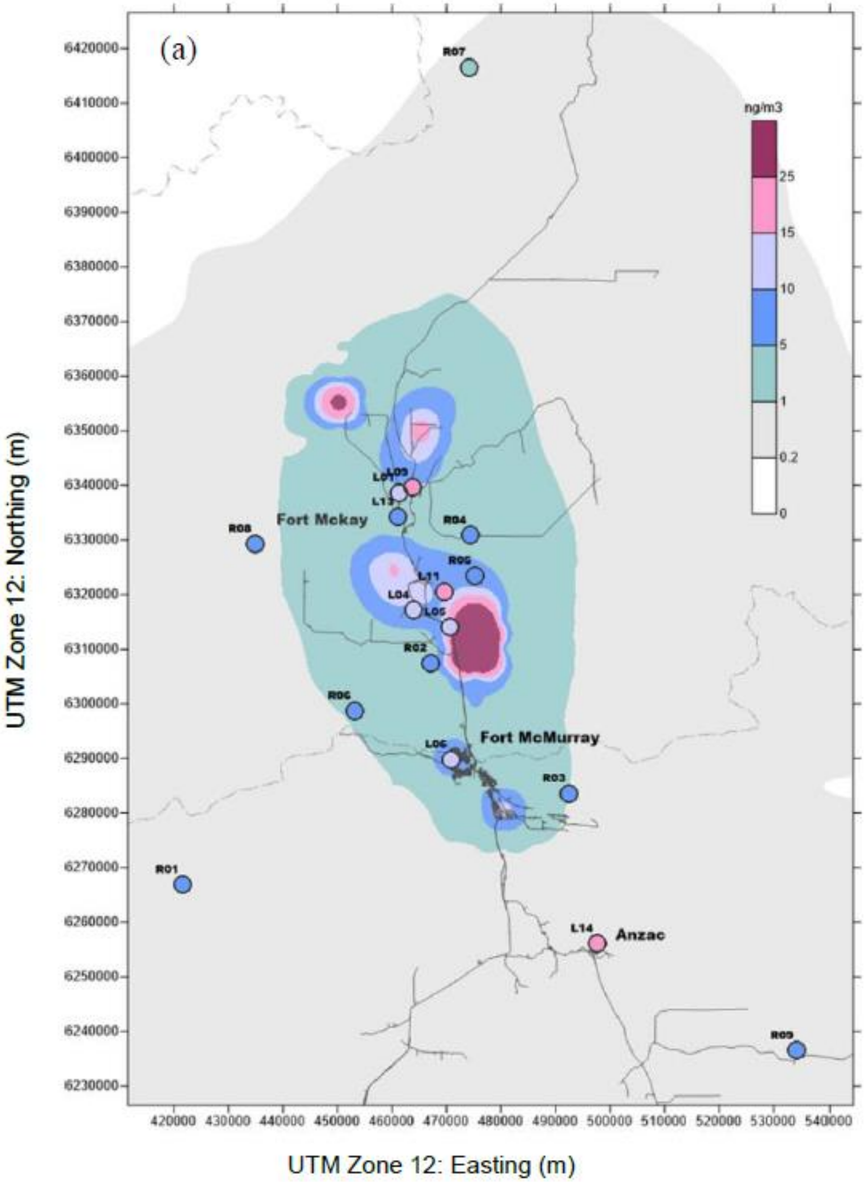

Figure 2(a): Average model-predicted PAH concentration contours using CEMA-derived emissions overlaid with passive measurements from November 2010 to June 2012 (circles)

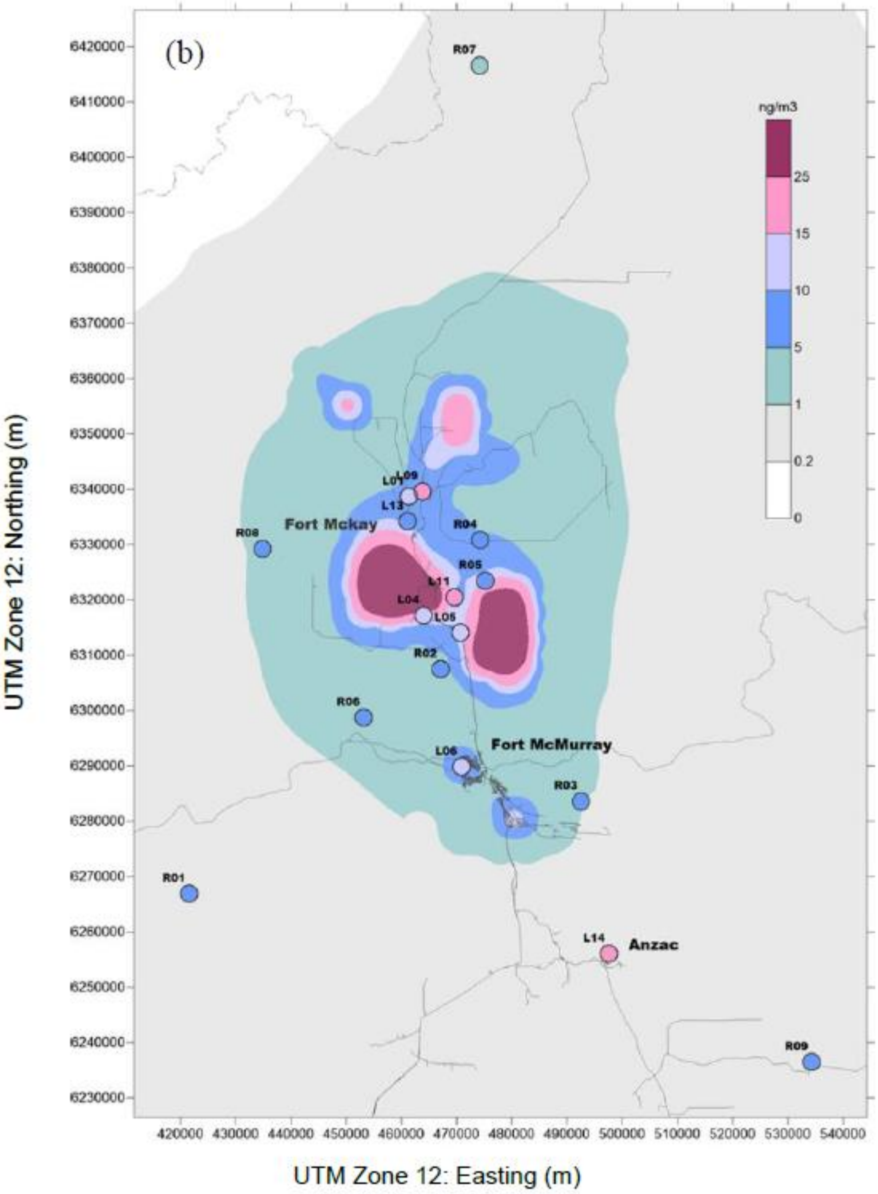

Figure 2(b):~~.~~ Average model-predicted PAH concentration contours using JOSM-derived emissions overlaid with passive measurements from November 2010 to June 2012 (circles)

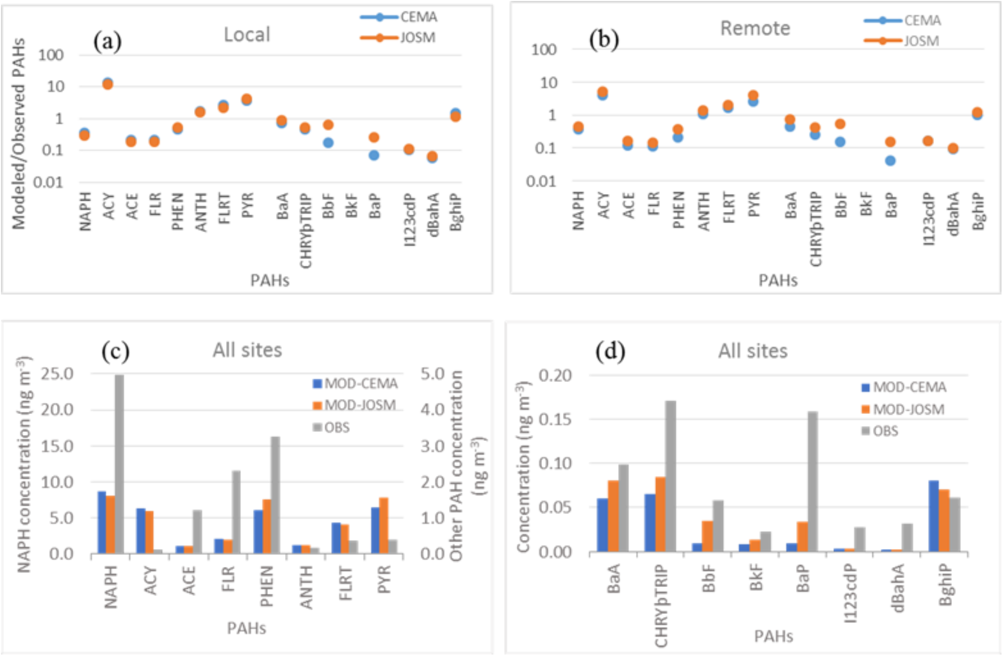

Figure 3:~~-~~ The ratios of CEMA and JOSM modelled concentrations to observed concentrations of speciated PAHs at local (a) and remote (b) sites. Comparison of average CEMA and JOSM modelled concentrations and observed concentrations at all sites (c,d). Note the different y-axis scales for the concentrations in figures c and d.

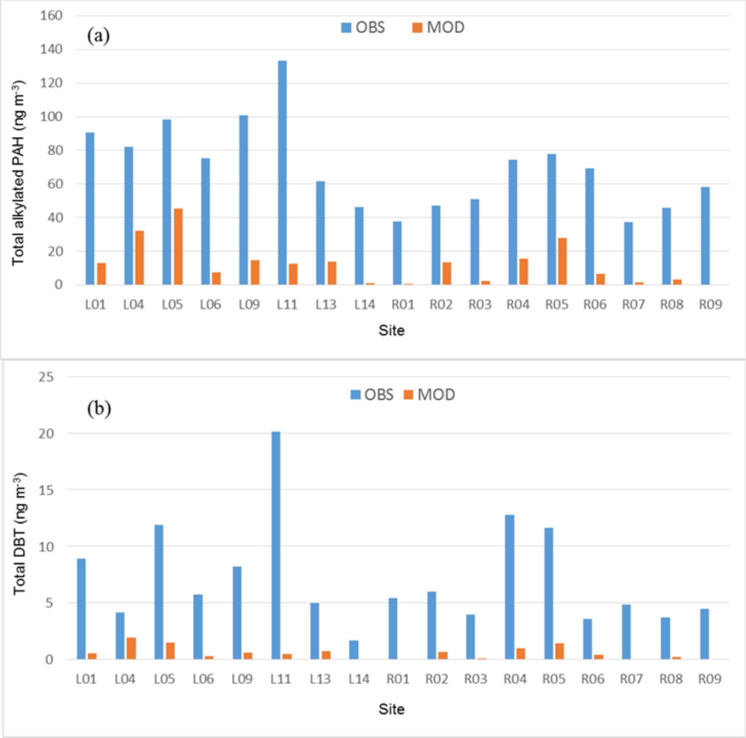

Figure 4:~~.~~ Comparison of average concentrations of total alkylated PAHs (a) and DBTs (b) between passive sampling observations and model using JOSM-derived emissions database.

Supplementary Material

Emissions databases for polycyclic aromatic compounds in the Canadian Athabasca Oil Sands Region – development using current knowledge and evaluation with passive sampling and air dispersion modelling data

Xin Qiu[1], Irene Cheng[2], Fuquan Yang[1], Erin Horb[3], Leiming Zhang[2], Tom Harner[2]

[1]Novus Environmental Inc., Guelph, Ontario, N1G 4T2, Canada
[2]Air Quality Research Division, Science and Technology Branch, Environment and Climate Change Canada, Toronto, Ontario, M3H 5T4, Canada
[3]Novus Environmental Inc., Calgary, Alberta, T2R 1K7, Canada

Correspondence to: Xin Qiu (xinq@novusenv.com) and Leiming Zhang (leiming.zhang@canada.ca)

Contents:

S1. PAC emissions estimation and speciation methodology

S2. CALPUFF model configuration

Table S1. VOC emissions used to calculate PAC emissions

Table S2. Comparisons of model performance between JOSM-derived and CEMA-derived PAH emissions and over local and remote sites.

Tables S3 to S10. PAC emissions estimates and speciation profiles

Tables S11 to S28. Model features, domain and input parameters

Figure S1. Map of tailings pond locations in the CEMA and JOSM emissions databases, oil sands operations, and PAC passive air monitoring locations

Figure S2. Map of the model domain and the study area

Figure S3. Map of unsubstituted PAH emissions in the AOSR

Figure S4: Fire radiative power distribution in the AOSR

Figure S5. Model sensitivity analysis on the impact of point and line (transportation) source emissions (PAHs_mod) on total PAH concentrations at 17 passive sampling sites (PAHs_obs)

S1 PAC emissions estimation and speciation methodology

S1.1 Tailings ponds

The PAH emission speciation profiles for oil sands tailings ponds is based on the paper by Galarneau et al. (2014). This study reported 1,069 kg/year emissions from tailings ponds for 13 PAH species during the JOSM field campaign (2011-2013). Based on the relative flux contributions among PAH species in Galarneau's paper, phenanthrene and pyrene dominated tailings pond PAH emissions. In our modelling practice, phenanthrene was given 50% mass fraction weight factor and pyrene was given 30% although they are not explicitly quantified in the paper. The remaining 20% weight factors are evenly distributed among the remaining 11 PAH species. As Galarneau et al. (2014) did not quantify naphthalene, acenaphthylene and acenaphthene, we do not include them in the tailings pond PAH emission. Although acenaphthylene and acenaphthene were excluded in tailings pond emissions, both of them are quantified in other PAH emission sources, such as mine fleet and point sources; therefore, they are included in total PAH emissions. However, in our study, we intentionally excluded naphthalene (NAPH) in our statistical analysis in the main paper due to its higher concentration and uncertainties compared with other PAHs species. This may lead to a bias in the modelling performance of total PAHs. Table S3 summarizes the PAH speciation profiles of tailings pond emissions. The profiles are presented as mass fractions of total PAHs.

In order to develop individual tailings pond PAH emissions for the JOSM-derived emissions database, we propagated the total annual PAH amount to each of the tailings ponds using the area size fraction of each pond and the PAH profiles in Table S3. Table S4 summarizes JOSM tailings pond total PAH emissions and the areas of each tailings pond.

The JOSM database tailings pond polygon areas in Table S4 were estimated from JOSM nonpoint emission source database shapefiles. Based on the coordinates of pond polygons, we calculated the areas of all tailings ponds. Environment and Climate Change Canada's JOSM emissions database files are available online (ECCC, 2016). The CEMA database tailings pond polygon areas in Table S5 were estimated from CEMA nonpoint emission source database files (Vijayaraghavan et al, 2010). We estimated CEMA tailings pond areas using the polygon coordinates supplied in the emissions files. Note that the pond numbers in Table S4 from JOSM are different from those in Table S5 from CEMA. Figure S1 shows the layouts of tailings ponds in the CEMA and JOSM emissions databases.

To maintain consistency in CEMA PAH emissions from tailings ponds, we estimated total tailings PAHs from CEMA by multiplying the JOSM tailings pond PAH total emissions with VOC emission ratios (of emission values from the two inventories), and then applied CEMA pond area size factors for individual ponds, as shown in Table S5.

S1.2 Mine face

There were no measurements of PAHs over oil sands mine face sources available at the time of this study. We made the assumption that PAH species emitted from mine faces should be similar to tailings ponds; thus the speciation profile of tailings pond PAH emissions in Table S3 was used for mine faces. However, PAH emissions intensity was assumed to be less than tailings ponds due to the fact that the total JOSM VOC emissions amount from mine face sources was only approximately 40% of that from tailings ponds (Table S1), although their areas were very close (tailings pond was 182.60 km^2 and mine face was 170.11 km^2). We also assumed that the PAH emission rates (unit: $g/s/m^2$) from mine faces were half of the rates from tailings ponds. In Tables S6 and S7, total PAH emissions from mine face sources were obtained by multiplying the PAH emission rate, the polygon area, and emissions duration (time) for CEMA and JOSM mines, respectively.

CEMA mine face polygon areas in Table S6 were estimated from CEMA nonpoint emissions database files (Vijayaraghavan et al, 2010). We estimated CEMA mine face areas with their polygon coordinates supplied in the emission files. Similarly, the JOSM mine face polygon areas in Table S7 were estimated from JOSM nonpoint emissions database shapefiles. We first estimated the coordinates of mine face polygons and then calculated their areas.

S1.3 Mine fleet

PAH emissions from mine fleet sources were speciated by mass fraction of total VOC emissions from mine fleet. The PAH speciation profiles were based on the CEMA study by Vijayaraghavan et al. (2010). If the total VOC emission rate is known, emissions of individual VOC and PAH compound groups can be calculated using the EPA SPECIATE database (USEPA, 2017). This EPA database provides the mass fraction of various hydrocarbon compounds. Note that the dominant species in mine fleet PAH emissions is naphthalene, which is not quantified in tailings pond emissions. Table S8 summarizes the PAH mass fractions of mine fleet VOCs. Tables S9 and S10 present PAH emissions for CEMA and JOSM mine fleet emissions, respectively. The CEMA mine fleet polygon areas in Table S9 were estimated from CEMA nonpoint emission source database files (Vijayaraghavan et al., 2010). The VOC emissions for mine fleet in the CEMA database were provided as both fleet area polygons and emissions for each of the 11 polygons. In the JOSM database, VOC emissions from mine fleet were provided as a facility total for each of the six facilities. Each facility was assigned one or more mine fleet polygon areas, and then the VOC emissions for each facility was distributed between the mine fleet polygon areas for a given facility. Note that the JOSM mine fleet polygon areas in Table S10 used the same polygon areas as mine face sources. This assumption is based on the fact that all the mine faces are covered by the operating mine fleet vehicles and infrastructure.

S1.4 Point sources, transportation, residential and area sources

In this study, CEMA PAH emissions (Vijayaraghavan et al., 2010) were used for oil sands modeling. Note that the majority of CEMA speciation profiles were based on a series of EIA studies in the oil sands area. Details can be found in the CEMA report (Vijayaraghavan et al., 2010). For the sources that are not available in CEMA database, PAH species were estimated based on SPECIATE, the EPA's repository of organic and PM speciation profiles of air pollution sources (Simon et al., 2010). The profiles can be used to create speciated emissions inventories for ozone modelling (e.g. NO, NO2, and explicit VOC species) and to estimate hazardous and toxic air pollutant emissions from total PM and organic primary emissions. PAH species, such as acenaphthene, acenaphthylene, fluoranthene, etc., are available for the most common emission source types. Note that the SPECIATE database only contains profiles for typical sources operated in the U.S.; thus, speciation profiles may not be available for certain sources operated in northeastern Alberta, such as oil sands facilities. The current version of the SPECIATE database is 4.5.

S1.5 Alkylated and DBT emissions

There is a lack of alkylated PAH and DBT speciation profiles from oil sands studies. U.S. EPA's SPECIATE program does not include oil sands related alkylated PAH species except mobile sources, such as mine fleet. In this study, we included mine fleet emissions profiles and estimated alkylated PAHs from mine fleet and transportation line sources. In addition, we roughly estimated alkylated PAHs and DBTs from tailings ponds indirectly based on the observed PAHs and alkylated PAHs, plus the observed tailings pond PAH emissions from Sect. S1. We made an assumption that the ratio (*R*) between total PAH emissions and total alkylated PAHs or DBTs emissions from tailings ponds is equivalent to the ratio of average PAHs concentration and average alkylated PAHs or DBTs concentration at all 17 passive monitoring sites (Fig. S1b; Schuster et al., 2015). In this sense, the total alkylated PAHs and DBTs emissions from tailings ponds can be calculated from the known PAH emissions from tailings ponds divided by the ratio, *R*. Regarding alkylated PAHs and DBTs emissions profiles (i.e., the percentage mass fraction for each of the species), it was assumed to be equivalent to the observed alkylated PAHs and DBTs speciation profiles of the 17 passive monitoring sites.

S2 CALPUFF model configuration

CALPUFF (Scire et al., 2000) is a multi-layer, multi-species, non-steady-state puff dispersion model that can simulate the effects of meteorological conditions, which vary with time and space, on pollutant transport, transformation, and deposition. CALPUFF can use the three-dimensional meteorological fields developed by the CALMET model, or simple, single-station winds in a format consistent with the meteorological files used to drive the ISCST3 steady-state Gaussian model. Details on CALPUFF and model guidance were obtained from AENV (2003), AESRD (2013), CEMA (2011), Lott (1984), Malm (2000), Scire et al. (2000), New Zealand Ministry of the Environment (2004), and USEPA (1995).

The major features and options of the CALPUFF model are summarized in Table S11. Some of the technical algorithms of relevance include:

- Wet and Dry Deposition: Not modelled in this study.

- Chemical Transformation: CALPUFF includes options to parameterize chemical transformation effects using the five-species scheme employed in the MESOPUFF II model, a modified six-species scheme adapted from the RIVAD/ARM3 method, or a set of user-specified, diurnally varying transformation rates.
- Building Downwash: The Huber-Snyder and Schulman-Scire downwash models are both incorporated into CALPUFF. An option is provided to use either model for all stacks, or make the choice on a stack-by-stack and wind-sector-by-wind-sector basis. Both algorithms have been implemented in such a way as to allow the use of wind-direction specific building dimensions. In addition, there is an option to use PRIME (Plume Rise Model Enhancements) as the method of calculating building downwash. PRIME includes two important features in downwash calculations: (1) enhanced plume dispersion coefficients due to turbulent wake effects, and (2) reduced plume rise due to descending streamlines and increased entrainment in the wake of the building.
- Dispersion Coefficients: Several options are provided in CALPUFF for the computation of dispersion coefficients: the use of turbulence measurements (σv and σw); the use of similarity theory to estimate σv and σw from modelled surface heat and momentum fluxes; the use of Pasquill-Gifford (PG) or McElroy-Pooler (MP) dispersion coefficients; or dispersion equations based on the Complex Terrain Dispersion Model (CDTM). Options are provided to apply an averaging-time correction or surface roughness length adjustments to the PG coefficients.

Model domain

The CALPUFF model requires the user to define locations where concentrations are to be calculated. The CALPUFF model domain (Table S12) was selected as 404 km by 580 km area at 4 km grid resolution in order to include a number of sources which might have the potential for impacting the selected Study Area (SA) of Alberta Oil Sands.

Meteorology

CALMET output was used to provide representative wind, temperature and turbulence fields. The three-dimensionally varying fields account for seasonal land-use differences.

Model options

The CALPUFF control file defines the 17 input groups as identified in Table S13. For many of the options, the default values were used in the absence of site/project specific data. Tables S14 to S28 identified the input parameters and the default options. Note that in the tables, values indicated by an asterisk (*) were allowed to vary spatially across the domain and were obtained from CALMET. A dash (-) indicates that the parameter was not applicable.

Table S1. Comparison of VOCs emissions (tonnes yr^{-1}) between CEMA and JOSM databases over the model domain. Data from ECCC (2016) and ECCC and AEP (2016).

Sources	CEMA 2010	JOSM 2013
Tailings pond	10,458	26,783
Mine face	3,655	10,053
Mine fleet	2,552	2,585
Residential and commercial	62	62
Non-industry (local traffic and airport)	26	26
Point sources[1]	5,092	5,092
Line sources	1,313	1,313

[1] Includes large upstream oil and gas (UOGs) but not small UOGs because most of them are outside the oil sands mining area and there are only a few of them

Table S2. Comparisons of model performance between JOSM-derived and CEMA-derived PAH emissions and over local and remote sites.

Local Sites			
PAHs	Monitored	Modeled-JOSM Emissions	Modeled-CEMA Emissions
Mean concentration (ng/m^3)	7.9	7.2	6.7
Percentage Error	-	17.1%	30.2%
RMSE (ng/m^3)	-	1.7	3.4
Remote Sites			
PAHs	Monitored	Modeled-JOSM Emissions	Modeled-CEMA Emissions
Mean concentration (ng/m^3)	4.8	2.5	1.7
Percentage Error	-	65.8%	67.1%
RMSE (ng/m^3)	-	3.6	3.5

RMSE: root mean square error

Table S3. Profile of PAH species in total tailings pond PAHs emissions

Species Name	Percentage of total PAH mass fraction (%)
Acenaphthene	0.0
Acenaphthylene	0.0
Anthracene	1.82
Benz[a]anthracene	1.82
Benzo[a]pyrene	1.82
Benzo[b]fluoranthene	1.82
Benzo[ghi]perylene	1.82
Benzo[k]fluoranthene	1.82
Chrysene	1.82
Dibenz[a,h]anthracene	1.82
Fluoranthene	1.82
Fluorene	1.82
Indeno[1,2,3-cd]pyrene	1.82
Naphthalene	0.0
Phenanthrene	50.0
Pyrene	30.0

Table S4. PAH emissions of tailings ponds from JOSM-derived emissions database

Polygon Name	Area(km^2)	PAH(kg/year)
Pond JOSM1	18.27	106.95
Pond JOSM2	1.48	8.65
Pond JOSM3	3.25	19.02
Pond JOSM4	1.71	9.99
Pond JOSM5	0.59	3.48
Pond JOSM6	1.46	8.57
Pond JOSM7	2.83	16.59
Pond JOSM8	6.86	40.16
Pond JOSM9	2.98	17.44
Pond JOSM10	7.76	45.45
Pond JOSM11	12.31	72.09
Pond JOSM12	0.43	2.50
Pond JOSM13	18.76	109.83
Pond JOSM14	28.42	166.40
Pond JOSM15	9.82	57.49
Pond JOSM16	4.83	28.26
Pond JOSM17	3.66	21.41
Pond JOSM18	13.22	77.97
Pond JOSM19	7.54	44.12
Pond JOSM20	1.80	10.54
Pond JOSM21	21.64	126.71

Pond JOSM22	8.31	48.63
Pond JOSM23	3.56	20.85
Pond JOSM24	1.01	5.88

Table S5. PAH emissions of tailings ponds from the CEMA-derived emissions database

Polygon Name	**Area(km^2)**	**PAH(kg/year)**
Pond CEMA1	7.5	35.68
Pond CEMA2	16.9	80.39
Pond CEMA3	3.04	14.46
Pond CEMA4	0.64	3.04
Pond CEMA5	1.6	7.61
Pond CEMA6	1.96	9.32
Pond CEMA7	3.24	15.41
Pond CEMA8	4.41	20.98
Pond CEMA9	1.44	6.85
Pond CEMA10	13.5	64.22
Pond CEMA11	11.5	54.70
Pond CEMA12	10.2	48.52
Pond CEMA13	6.25	29.73
Pond CEMA14	1.96	9.32
Pond CEMA15	3.61	17.17

Table S6. PAH emissions from each mine face of the CEMA-derived emissions database

Polygon Name	**Area(km^2)**	**PAH(kg/year)**
Mine Face CEMA1	1.21	1.66
Mine Face CEMA2	4.50	6.19
Mine Face CEMA3	11.52	15.9
Mine Face CEMA4	6.0	8.26
Mine Face CEMA5	8.14	11.2
Mine Face CEMA6	3.68	5.06

Table S7. PAH emissions from each mine face of the JOSM-derived emissions database

Polygon Name	**Area(km^2)**	**PAH(kg/year)**
Mine Face JOSM1	8.68	30.59
Mine Face JOSM2	3.53	12.44
Mine Face JOSM3	7.32	25.80
Mine Face JOSM4	3.24	11.42
Mine Face JOSM5	12.14	42.78
Mine Face JOSM6	4.97	17.52
Mine Face JOSM7	16.03	56.49
Mine Face JOSM8	4.31	15.19

Mine Face JOSM9	2.65	9.34
Mine Face JOSM10	8.59	30.27
Mine Face JOSM11	14.55	51.28
Mine Face JOSM12	17.46	61.53
Mine Face JOSM13	2.11	7.44
Mine Face JOSM14	25.90	91.28
Mine Face JOSM15	38.65	136.21

Table S8. Profile of PAH species as a mass fraction of total mine fleet VOCs

Species Name	Percentage of total VOC mass (%)
Acenaphthene	0.007360883
Acenaphthylene	0.026735644
Anthracene	0.0004767412
Benz[a]anthracene	0.0001136551
Benzo[a]pyrene	0.0
Benzo[b]fluoranthene	0.0
Benzo[ghi]perylene	0.002219707
Benzo[k]fluoranthene	0.0
Chrysene	0.001277666
Dibenz[a,h]anthracene	0.0
Fluoranthene	0.020213825
Fluorene	0.013196195
Indeno[1,2,3-cd]pyrene	0.0
Naphthalene	0.235319433
Phenanthrene	0.035507681
Pyrene	0.027422151

Table S9. PAH emissions of mine fleet from the CEMA-derived emissions database

Polygon Name	Area(km^2)	PAH(kg/year)
Mine Fleet CEMA1	4.5	2449.81
Mine Fleet CEMA2	0.06	68.47
Mine Fleet CEMA3	1.21	501.11
Mine Fleet CEMA4	0.06	2.84
Mine Fleet CEMA5	0.05	9.49
Mine Fleet CEMA6	0.02	27.92
Mine Fleet CEMA7	0.08	46.19
Mine Fleet CEMA8	11.52	4399.22
Mine Fleet CEMA9	6.00	822.32
Mine Fleet CEMA10	8.14	1115.34
Mine Fleet CEMA11	3.68	130.36

Table S10. PAH emissions of mine fleet from the JOSM-derived emissions database

Polygon Name	Area(km^2)	PAH(kg/year)
Mine Fleet JOSM1	8.68	501.45
Mine Fleet JOSM2	3.53	279.51
Mine Fleet JOSM3	7.32	302.78
Mine Fleet JOSM4	3.24	133.88
Mine Fleet JOSM5	12.14	501.84
Mine Fleet JOSM6	4.97	205.63
Mine Fleet JOSM7	16.03	662.78
Mine Fleet JOSM8	4.31	178.12
Mine Fleet JOSM9	2.65	109.39
Mine Fleet JOSM10	8.59	355.39
Mine Fleet JOSM11	14.55	882.11
Mine Fleet JOSM12	17.46	1058.21
Mine Fleet JOSM13	2.11	127.69
Mine Fleet JOSM14	25.90	1765.20
Mine Fleet JOSM15	38.65	2633.99

Table S11. Major features of the CALPUFF Model

Source Types	Point sources (constant or variable emissions) Line sources (constant or variable emissions) Volume sources (constant or variable emissions) Area sources (constant or variable emissions)
Non-steady-state emissions and meteorological conditions	Gridded 3-D fields of meteorological variables (winds, temperature) Spatially variable fields of mixing height, friction velocity scale, Monin-Obukhov length, precipitation rate Vertically and horizontally varying turbulence and dispersion rates Time-dependant source and emissions data
Efficient sampling functions	Integrated puff formulation Elongated puff (slug) formulation
Dispersion coefficient (σy,σz) options	Direct measurements of σv and σw Estimated values of σv and σw based on similarity theory Pasquill-Gifford (PG) dispersion coefficients (rural areas) McElroy-Pooler (MP) dispersion coefficients (rural areas) CTDM dispersion coefficients (neutral / stable) PDF formulation for the convective boundary layer
Vertical wind shear	Puff splitting Differential advection and dispersion
Plume rise	Partial penetration Buoyant and momentum rise Stack tip effects Vertical wind shear Building downwash effects
Building downwash	Huber-Snyder method Schulman-Scire method
Sub-grid Scale Complex Terrain	CTDM flow module Dividing streamline, Hd - Above Hd puff flows over the hill and experiences altered diffusion rates - Below Hd puff deflects around the hill, splits, and wraps around the hill

Interface to the Emissions Production Model (EPM)	Time-varying heat flux and emissions from controlled burns and wildfires
Dry Deposition	Not modelled in this study
Over Water and Coastal Interaction Effects	Over water boundary layer parameters Abrupt change in meteorological conditions, plume dispersion at coastal boundary Plume fumigation Option to introduce sub-grid scale Thermal Internal Boundary Layers (TIBL's) into coastal grid cells
Chemical Transformation Options	Pseudo-first-order chemical mechanism for SO2, NOX, HNO3, and NO3 (MESOPUFF II method) Pseudo-first-order chemical mechanism for SO2, SO4, NO, NO2, HNO3 and NO3 (RIVAD/ARM3 method) User-specified diurnal cycles of transformation rates No chemical conversion
Wet Removal	Not modelled in this study
Graphical User Interface	Point-and-click set-up and data input Enhanced error checking of model inputs On-line Help files

Table S12. CALPUFF Model Domain Coordinates (UTM Zone 12; NAD 83) (404 km x 580 km grid)

Domain Extent	Easting (km)	Northing (km)
Southwest	306.219	6054.418
Northwest	306.219	6634.418
Southeast	710.219	6054.418
Northeast	710.219	6634.418

Table S13. Input Groups in the CALPUFF Control File

Input Group	Description	Applicable to the Project
0	Input and output file names	Yes
1	General run control parameters	Yes
2	Technical options	Yes
3	Species list	Yes
4	Grid control parameters	Yes
5	Output options	Yes
6	Sub grid scale complex terrain inputs	No
7	Dry deposition parameters for gases	No
8	Dry deposition parameters for particles	No
9	Miscellaneous dry deposition for parameters	No
10	Wet deposition parameters	No
11	Chemistry parameters	Yes
12	Diffusion and computational parameters	Yes

13	Point source parameters	Yes
14	Area source parameters	Yes
15	Line source parameters	No
16	Volume source parameters	No
17	Discrete receptor information	Yes

Table S14. CALPUFF Model Options Group 1 (Input Group 1: General run control parameters)

Parameter	Default	Project	Comments
METRUN	0	0	All model periods in met file(s) will be run
IBYR	-	2010	Starting year
IBMO	-	10	Starting month
IBDY	-	1	Starting day
IBHR	-	1	Starting hour
IRLG	-	19752	Length of run (from Oct 2010 to the end of 2012)
XBTZ	-	7	Base time zone
NSPEC	5	16	Number of chemical species
NSE	3	16	Number of chemical species to be emitted
ITEST	2	2	Program is executed after SETUP phase
Input Group 1: General run control parameters (Continued)			
Parameter	**Default**	**Project**	**Comments**
MRESTART	0	0	Does not read or write a restart file
NRESPD	0	0	Restart file written every NRESPD period
METFM	1	1	CALMET binary file (CALMET.MET)
AVET	60	60	Averaging time in minutes
PGTIME	60	60	PG Averaging time in minutes

Table S15. CALPUFF Model Options Group 2 (Input Group 2: Technical Options)

Parameter	Default	Project	Comments
MGAUSS	1	1	Gaussian distribution used in near field
MCTADJ	3	3	Partial plume path terrain adjustment
MCTSG	0	0	Scale-scale complex terrain not modelled
MSLUG	0	0	Near-field puffs not modelled as elongated
MTRANS	1	1	Transitional plume rise modelled
MTIP	1	0	Stack tip downwash used

Parameter	Default	Project	Comments
MBDW	1	1	Building downwash simulated using PRIME method
MSHEAR	0	1	Vertical wind shear modelled
MSPLIT	0	0	Puffs are not split
MCHEM	0	0	Transformation rates computed internally using (RIVID/ARM3) scheme
MAQCHEM	0	0	Aqueous phase transformation not modelled
MWET	1	0	Wet removal not modelled
MDRY	1	0	Dry deposition not modelled
MDISP	3	2	PG dispersion coefficients from internally calculated sigma v, sigma w using micrometeorological variables (u*, v*, L, etc.)
MTURBVW	3	3	Use both σv and σw from PROFILE.DAT to compute σy and σz, (n/a)
MDISP2	3	3	PG dispersion coefficients from internally calculated sigma v, sigma w using micrometeorological variables (u*, v*, L, etc.)
MCTURB	1	1	Standard CALPUFF subroutines used to compute turbulence σv and σw
MROUGH	0	0	PG σy and σz adjusted for roughness
MPARTL	1	1	Partial plume penetration of elevated inversion
MTINV	0	0	Strength of temperature inversion computed from default gradients
MPDF	0	1	PDF used for dispersion under convective conditions
MSGTIBL	0	0	Sub-grid TIBL module not used for shoreline
MBCON	0	0	Boundary concentration conditions not modelled
MFOG	0	0	Do not configure for FOG model output
MREG	1	0	Do not test options specified to see if they conform to regulatory values

Table S16. CALPUFF Model Options Group 3 (Input Group 3: Species list-chemistry options)

CSPEC	Modelled (yes=1, no=0)	Emitted (yes=1, no=0)	Dry (0=none, 1=computed-gas, 2=computed particle, 3=user-specified)	Output group number
Naphthalene	1	1	1	0
Acenaphthylene	1	1	1	0
Acenaphthene	1	1	1	0
Fluorene	1	1	1	0
Phenanthrene	1	1	2	0
Anthracene	1	1	2	0
Fluoranthene	1	1	2	0
Pyrene	1	1	2	0
Benz(a)anthracene	1	1	2	0
Chrysene	1	1	2	0
Benzo(b)fluoranthene	1	1	2	0

Benzo(k)fluoranthene	1	1	2	0
Benzo(a)pyrene	1	1	2	0
Indeno(1,2,3-	1	1	2	0
Dibenz(a,h)anthracene	1	1	2	0
Benzo(g,h,i)perylene	1	1	2	0

Table S17. CALPUFF Model Options Group 4 (Input Group 4: Grid control parameter)

Parameter	Default	Project	Comments
NX	-	101	Number of X grid cells in meteorological grid
N		145	Number of Y grid cells in meteorological grid
NZ	-	10	Number of vertical layers in meteorological grid
DGRIDKM	-	4	Grid spacing (km)
ZFACE	-	0,20,40,80,160,300 600, 1000, 1500, 2200, 3000	Cell face heights in meteorological grid (m)
XORIGKM	-	306.219	Reference X coordinate for SW corner of grid cell (1,1) of meteorological grid (km)
YORIGKM	-	6054.418	Reference Y coordinate for SW corner of grid cell (1,1) of meteorological grid (km)
IUTMZN	-	12	UTM zone of coordinates
IBCOMP	-	1	X index of lower left corner of the computational grid
JBCOMP	-	1	Y index of lower left corner of the computational grids
IECOMP	-	101	X index of the upper right corner of the computational grid
JECOMP	-	145	Y index of the upper right corner of the computational grid
SAMP	T	F	Sampling grid is not used
IBSAMP	-	-	X index of lower left corner of the sampling grid
JBSAMP	-	-	Y index of lower left corner of the sampling grid
IESAMP	-	-	X index of upper right corner of the sampling grid
JESAMP	-	-	Y index of upper right corner of the sampling grid
MESHDN	1	1	Nesting factor of the sampling grid

Table S18. CALPUFF Model Options Group 5 (Input Group 5: Output Option)

Parameter	Default	Project	Comments
ICON	-	1	Output file CONC.DAT containing concentrations is created
IDRY	-	1	Output file DFLX.DAT containing dry fluxes is created
IWET	-	1	Output file WFLX.DAT containing wet fluxes is created
IVIS	-	0	Output file containing relative humidity data is not created
LCOMPRS	T	F	Perform data compression in output file

Parameter	Default	Project	Comments
IMFLX	0	0	Do not calculate mass fluxes across specific boundaries
IMBAL	0	0	Do not report mass balances
ICPRT	0	0	Do not print concentration fields to the output list file
IDPRT	0	0	Do not print dry flux fields to the output list file
IWPRT	0	0	Do not print wet flux fields to the output list file
ICFRQ	1	1	Concentration fields are printed to output list file every 1 hour
IDFRQ	1	1	Dry flux fields are printed to output list file every 1 hour
IWFRQ	1	1	Wet flux fields are printed to output list file every 1 hour
IPRTU	1	3	Units for line printer output are in $\mu g/m^3$ for concentration and $\mu g/m^2/s$ for deposition
IMESG	2	2	Messages tracking the progress of run are written on screen
LDEBUG	F	F	Logical value for debug output
IPFDEB	1	1	First puff to track
NPFDEB	1	1	Number of puffs to track
NN1	1	1	Meteorological period to start output
NN2	10	10	Meteorological period to end output

Table S19. CALPUFF Model Options Group 6 (Input Group 6: Sub Grid Scale Complex Terrain Inputs)

Parameter	Default	Project	Comments
NHILL	0	0	Number of terrain features
NCTREC	0	0	Number of special complex terrain receptors
MHILL	-	2	Input terrain and receptor data for CTSG hills input in CTDM format
XHILL2M	1.0	1.0	Conversion factor for changing horizontal dimensions to metres
ZHILL2M	1.0	1.0	Conversion factor for changing vertical dimensions to metres
XCTDMKM	-	0	X origin of CTDM system relative to CALPUFF coordinate system (km)
YCTDMKM	-	0	Y origin of CTDM system relative to CALPUFF coordinate system (km)

Table S20. CALPUFF Model Option Group 9 (Input Group 9: Miscellaneous Dry Deposition Parameters)

PAC dry deposition was not modelled in this study. The modelled air concentrations do not account for dry deposition.

Table S21. CALPUFF Model Option Group 10 (Input Group 10: Wet Deposition Parameters, scavenging coefficients, units: s^{-1})

PAC wet deposition was not modelled in this study. The modelled air concentrations do not account for wet deposition.

Table S22. CALPUFF Model Option Group 11 (Input Group 11: Chemistry Parameters)

Parameters	Default	Project	Comments
MOZ	1	0	Use monthly ozone values
BCKO3	80-	40	Monthly background ozone concentration (ppb)
BCKNH3	10	10	Monthly background ammonia concentration (ppb)
RNITE1	0.2	0.2	Night time NO2 loss rate in percent/hour
RNITE2	2	2	Night time NO_X loss rate in percent/hour
RNITE3	2	2	Night time HNO3 loss rate in percent/hour
MH202	1	1	Background H2O2 concentrations (Aqueous phase transformations not modelled)
BCKH202	-	-1.00	Background monthly H2O2 concentrations (Aqueous phase transformations not modelled)

Table S23. CALPUFF Model Option Group 12 (Input Group 12: Dispersion/Computational Parameters)

Parameters	Default	Project	Comments
SYDEP	550	550	Horizontal size of a puff in metres beyond which the time dependant dispersion equation of Heffter (1965) is used
MHFTSZ	0	0	Do not use Heffter formulas for sigma z
JSUP	5	5	Stability class used to determine dispersion rates for puffs above boundary layer
CONK1	0.01	0.01	Vertical dispersion constant for stable conditions
CONK2	0.1	0.1	Vertical dispersion constant for neutral/stable conditions
TBD	0.5	0.5	Use ISC transition point for determining the transition point between the Schulman-Scire to Huber-Snyder Building Downwash scheme
IURB1	10	10	Lower range of land use categories for which urban dispersion is assumed
IURB2	19	19	Upper range of land use categories for which urban dispersion is assumed
ILANDUIN	20	20	Land use category for modelling domain
XLAIIN	3.0	3.0	Leaf area index for modelling domain
ZOIN	0.25	0.25	Roughness length in metres for modelling domain
ISIGMAV	1	1	Sigma-v is read for lateral turbulence data
IMIXCTDM	0	0	Predicted mixing heights are used
XMXLEN	1.0	1.0	Maximum length of emitted slug in meteorological grid units
XSAMLEN	1.0	10.0	Maximum travel distance of slug or puff in meteorological grid units during one sampling unit
MXNEW	99	60	Maximum number of puffs or slugs released from one source during one time step
MXSAM	99	60	Maximum number of sampling steps during one time step for a puff or slug
NCOUNT	2	2	Number of iterations used when computing the transport wind for a

Parameters	**Default**	**Project**	**Comments**
			sampling step that includes transitional plume rise
SYMIN	1.0	1.0	Minimum sigma y in metres for a new puff or slug
SZMIN	1	1	Minimum sigma z in metres for a new puff or slug

Stability Class	Parameter	
	SVMIN	SWMIN
	Minimum turbulence (σv) (m/s)	Minimum turbulence (σw) (m/s)
A	0.5	0.2
B	0.5	0.12
C	0.5	0.08
D	0.5	0.06
E	0.5	0.03
F	0.5	0.016

CDIV	0.0, 0.0	0.0, 0.0	Divergence criteria for dw/dz in met cells
WSCALM	0.5	0.5	Minimum wind speed allowed for non-calm conditions (m/s)
XMAXZI	3000	3000	Maximum mixing height in metres
XMINZI	50	50	Minimum mixing height in metres
WSCAT		1.54	wind speed category 1 [m/s]
		3.09	wind speed category 2 [m/s]
		5.14	wind speed category 3 [m/s]
		8.23	wind speed category 4 [m/s]
		10.8	wind speed category 5 [m/s]
SL2PF	10	10	Slug-to-puff transition criterion factor equal to sigma y/length of slug

Input Group 12: Dispersion/Computational Parameters (Continued)

Parameters	**Default**	**Project**	**Comments**
PTG0	0.02	0.02	potential temperature gradient for E stability [K/m]
	0.035	0.035	potential temperature gradient for F stability [K/m]
NSPLIT	3	3	Number of puffs that result every time a puff is split
IRESPLIT	0,0,0,0,00,0,0, 0,0,0,0,0,0,0,0, 0,1,0,0,0,0,0,0	0,0,0,0,00,0,0,0,0, 0,0,0,0,0,0,0,1,0,0 ,0,0,0,0	Time(s) of day when split puffs are eligible to be split once again

Stability Class	Parameter	
	PLX0	PPC
	Wind speed profile exponent	Plume path coefficient
A	0.07	0.8
B	0.07	0.7
C	0.1	0.6
D	0.15	0.5
E	0.35	0.4
F	0.55	0.35

ZISPLIT	100	100	Minimum allowable last hour’s mixing height for puff splitting
ROLDMAX	0.25	0.25	Maximum allowable ratio of last hour’s mixing height and maximum mixing height experienced by the puff for puff splitting
NSPLITH	5	5	Number of puffs that result every time a puff is horizontally split
SYSPLITH	1	1	Minimum sigma-y of puff before it may be horizontally split
SHSPLITH	2	2	Minimum puff elongation rate due to wind shear before it may be horizontally split

Parameters	Default	Project	Comments
CNSPLITH	1.00E-07	0	Minimum concentration of each species in puff before it may be horizontally split
EPSSLUG	1.00E-04	0	Fractional convergence criterion for numerical SLUG sampling iteration
EPSAREA	1.00E-06	0	Fractional convergence criterion for numerical AREA sampling iteration
DRISE	1	1	Trajectory step length for numerical rise

Table S24. CALPUFF Model Option Group 13 (Input Group 13: Point Source Parameters)

Parameters	Default	Project	Comments
NPT1	-	689	Number of point sources with constant stack parameters or variable emission rate scale factors
IPTU	1	1	Units for point source emission rates are g/s
NSPT1	0	0	Number of source-species combinations with variable emissions scaling factors
NPT2	-	0	Number of point sources with variable emission parameters provided in external file

Table S25. CALPUFF Model Option Group 14 (Input Group 14: Area Source Parameters)

Parameters	Default	Project	Comments
NAR1	-	87	Number of polygon area sources
IARU	1	1	Units for point source emission rates are g/ m^2/s
NSAR1	0	880	Number of source-species combinations with variable emissions scaling factors
NAR2	-	0	Number of buoyant polygon area sources with variable location and emission parameters

Table S26. CALPUFF Model Option Group 15 (Input Group 15: Line Source Parameters)

Parameters	Default	Project	Comments
NLN2	-	-	Number of buoyant line sources with variable location and emission parameters
NLINES	-	29	Number of buoyant line sources
ILNU	1	1	Units for line source emission rates is g/s
NSLN1	0	0	Number of source-species combinations with variable emissions scaling factors.
MXNSEG	7	7	Maximum number of segments used to model each line
NLRISE	6	6	Number of distance at which transitional rise is computed
XL	-	22.81	Average line source length (m)
HBL	-	2.0	Average height of line source height (m)
WBL	-	10.0	Average building width (m)
WML	-	0.5	Average line source width (m)

DXL	-	2.0	Average separation between buildings (m)
FPRIMEL	-	50.0	Average buoyancy parameter (m4/s3)

Table S27. CALPUFF Model Option Group 16 (Input Group 16: Volume Source Parameters)

Parameters	Default	Project	Comments
NVL1	-	0	Number of volume sources
IVLU	1	1	Units for volume source emission rates is grams per second
NSVL1	0	0	Number of source-species combinations with variable emissions scaling factors
IGRDVL	-	-	Gridded volume source data is not used
VEFFHT	-	-	Effective height of emissions (m)
VSIGYI	-	-	Initial sigma y value (m)
VSIGZI	-	-	Initial sigma z value (m)

Table S28. CALPUFF Model Option Group 17 (Input Group 17: Discrete Receptor Information)

Parameters	Default	Project	Comments
NREC	-	9300	Number of non-gridded receptors

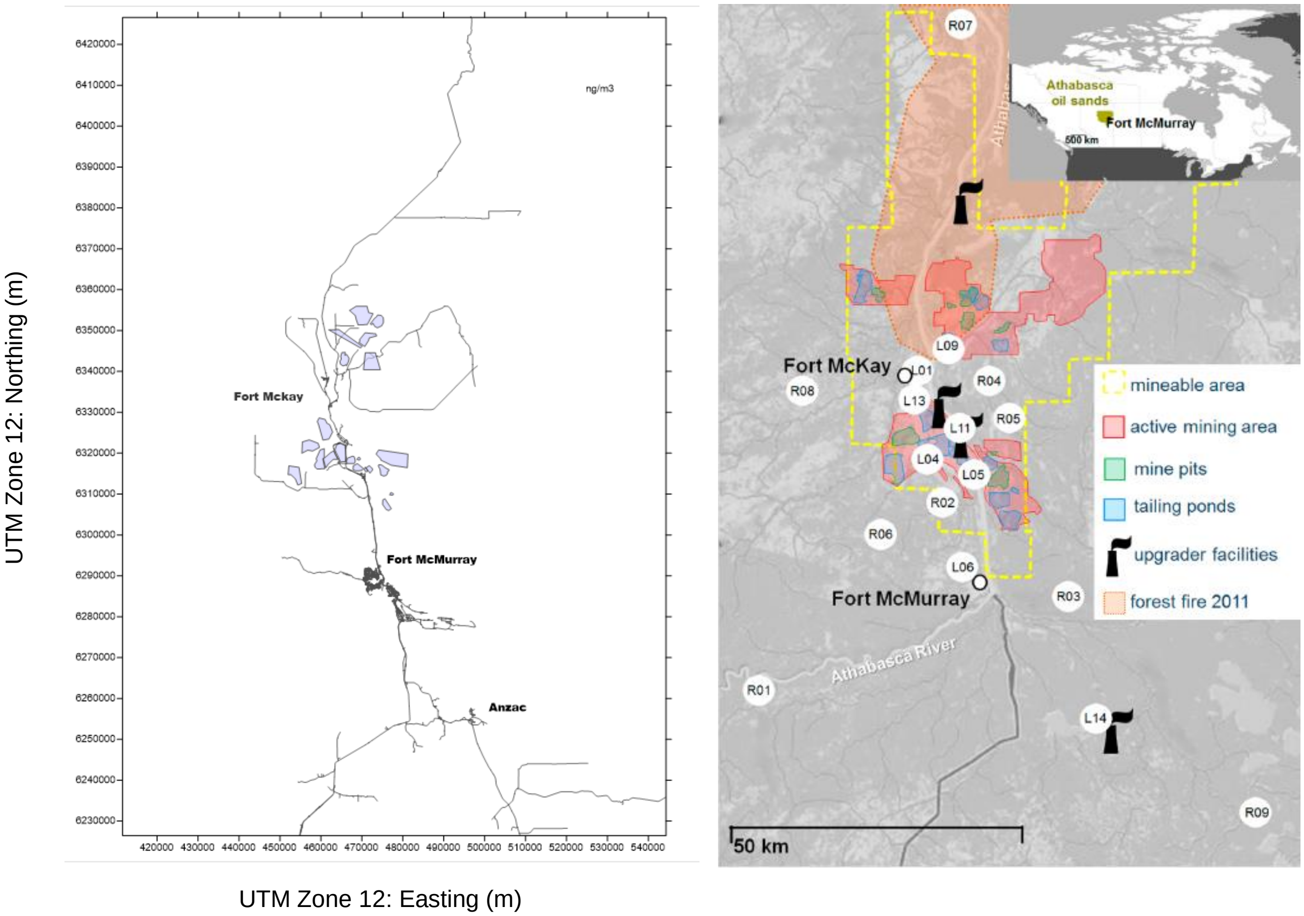

Figure S1. Map of tailings pond locations (shown in blue) in the CEMA emissions database (a) and PAC passive air monitoring locations from JOSM activities and oil sands operations obtained from Schuster et al. (2015) (b).

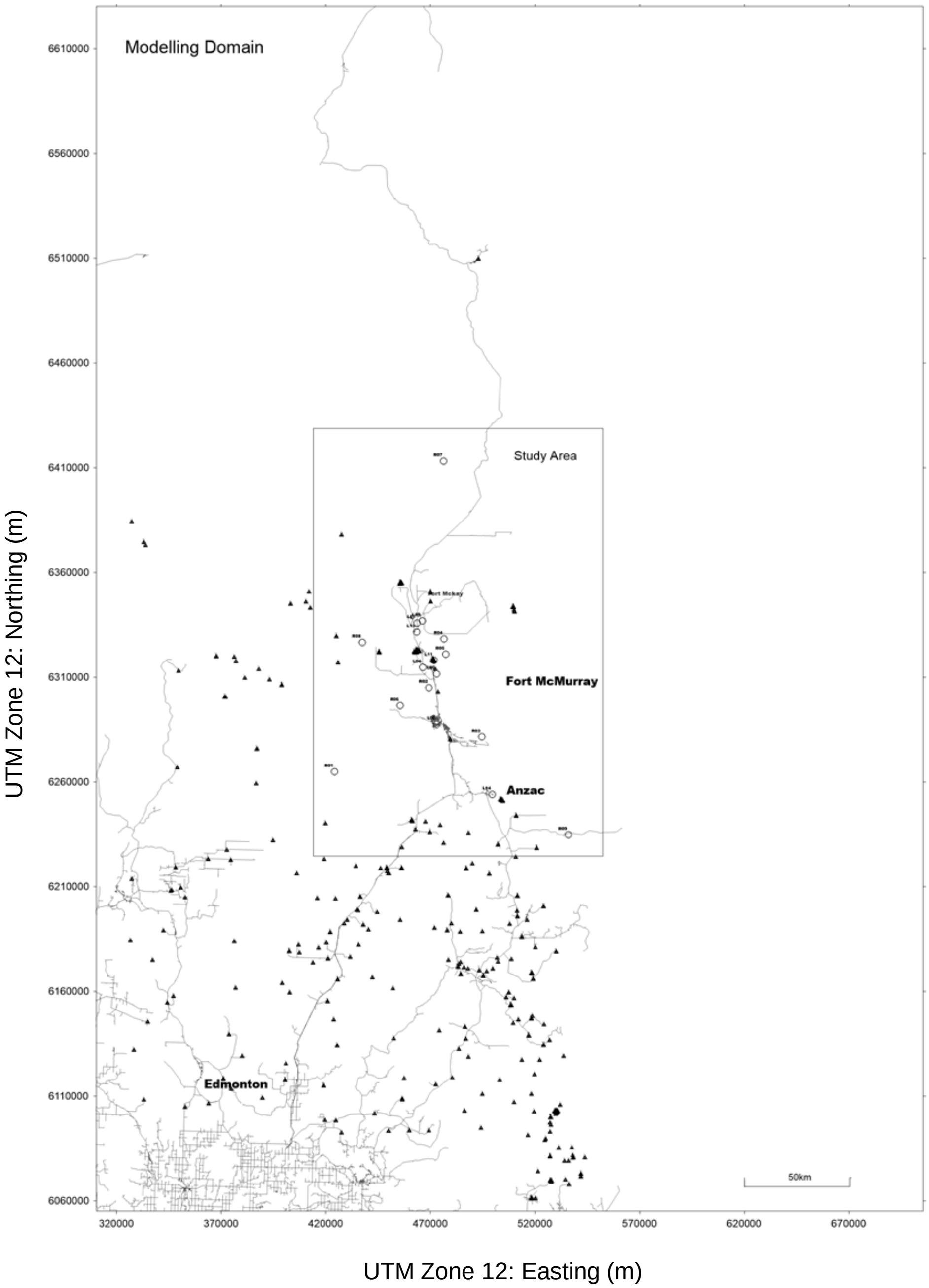

Figure S2. Map showing the point sources accounted for in the model domain and the study area where modelled concentrations are compared with measured air concentrations (Fig. S1). Black triangles indicate VOC point source locations are from the CEMA emissions database (Vijayarahavan et al., 2010) and the Capital Region Particulate Matter Air Modelling Assessment (Nopmongcol et al., 2014), which are converted to PAH emissions.

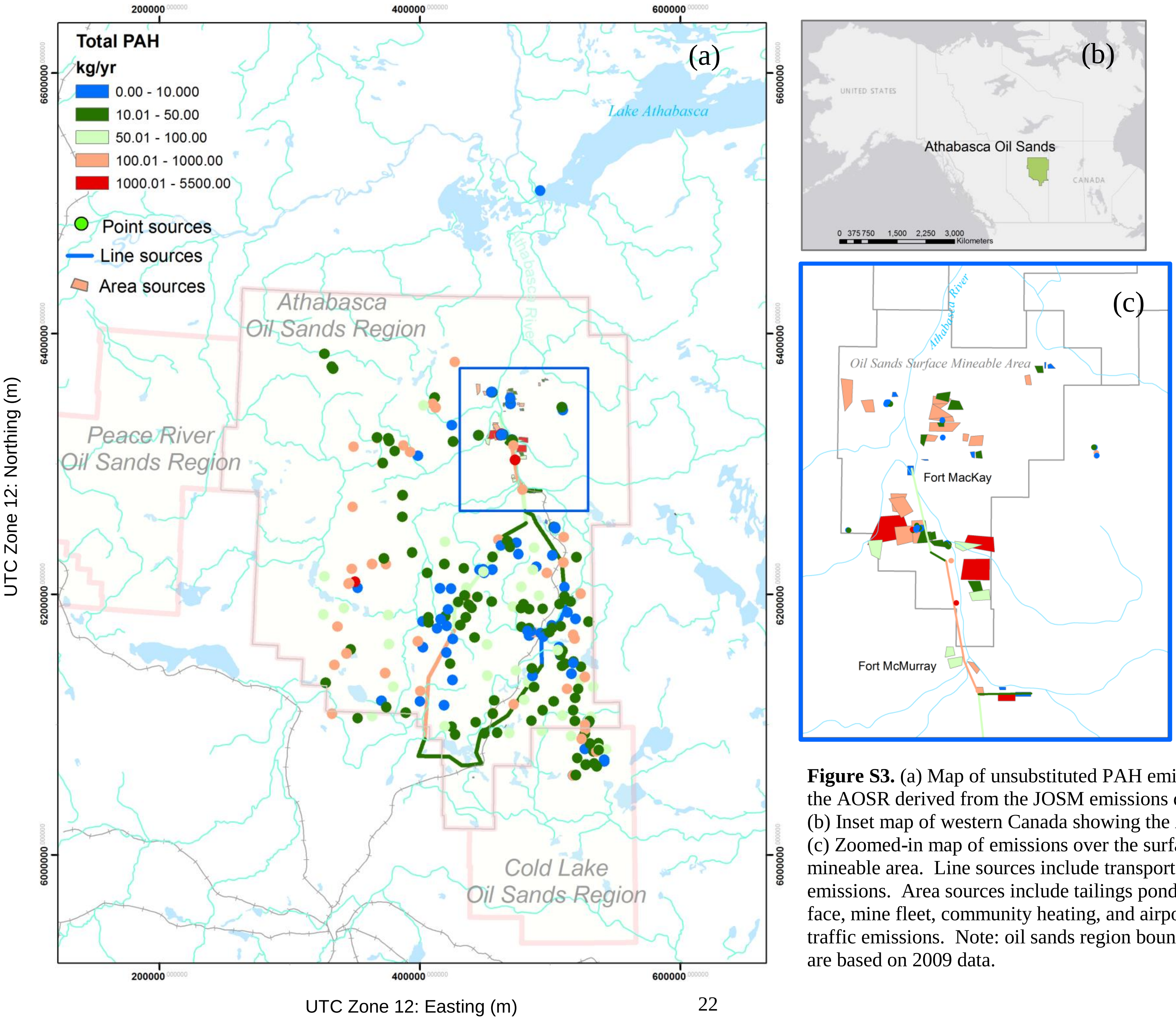

Figure S3. (a) Map of unsubstituted PAH emissions in the AOSR derived from the JOSM emissions database. (b) Inset map of western Canada showing the AOSR. (c) Zoomed-in map of emissions over the surface mineable area. Line sources include transportation emissions. Area sources include tailings pond, mine face, mine fleet, community heating, and airport and traffic emissions. Note: oil sands region boundaries are based on 2009 data.

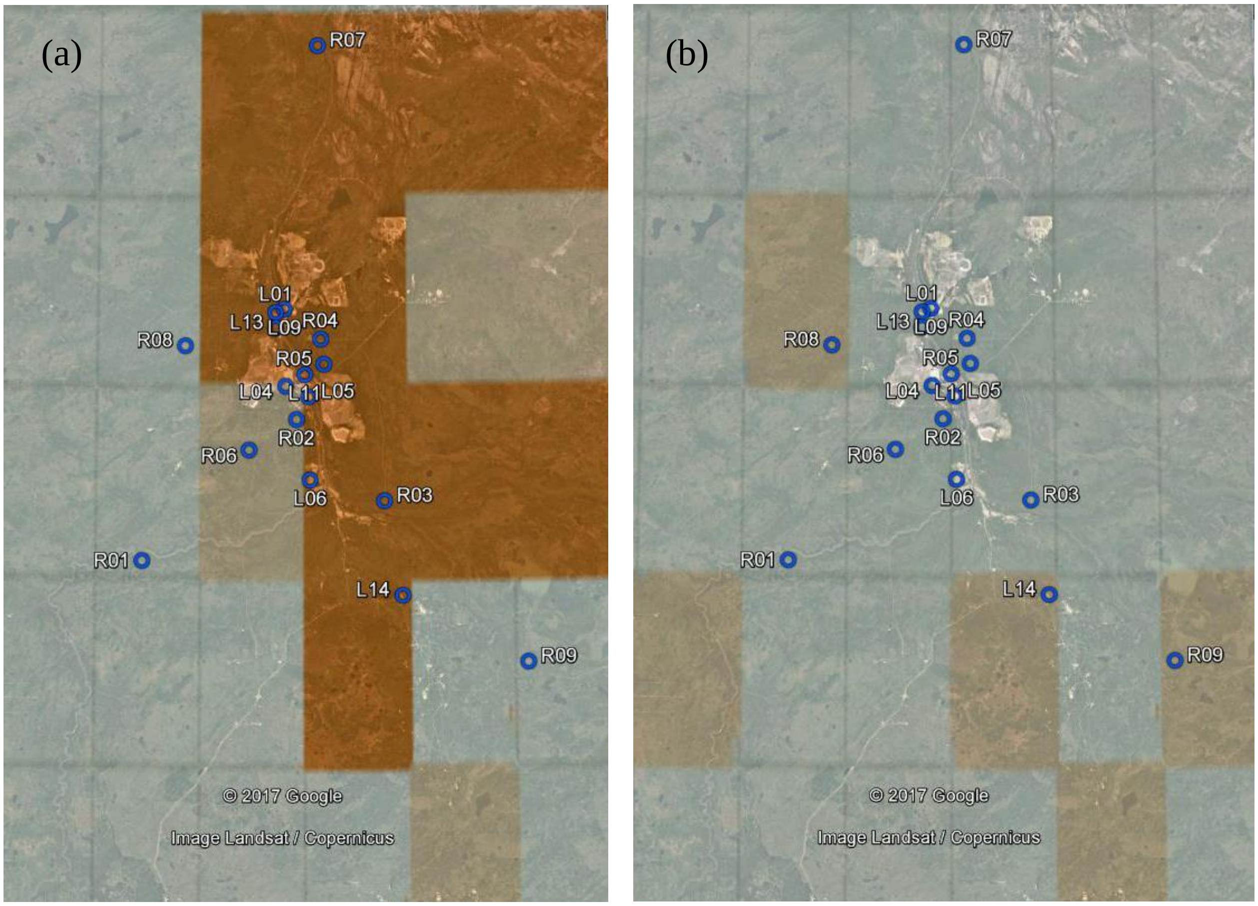

Figure S4. Mean fire radiative power (FRP in megawatts) during the active forest fire period from April 2011 to July 2011 (a) and excluding the April 2011 to July 2011 period in 2011 and 2012 (b). FRP is a measure of the intensity of biomass burning emissions; the data were obtained from MODIS (NASA, 2017). Dark orange: high intensity (80-220 MW); light orange: low intensity (10-39 MW); gray: zero intensity; blue circles: passive air monitoring sites.

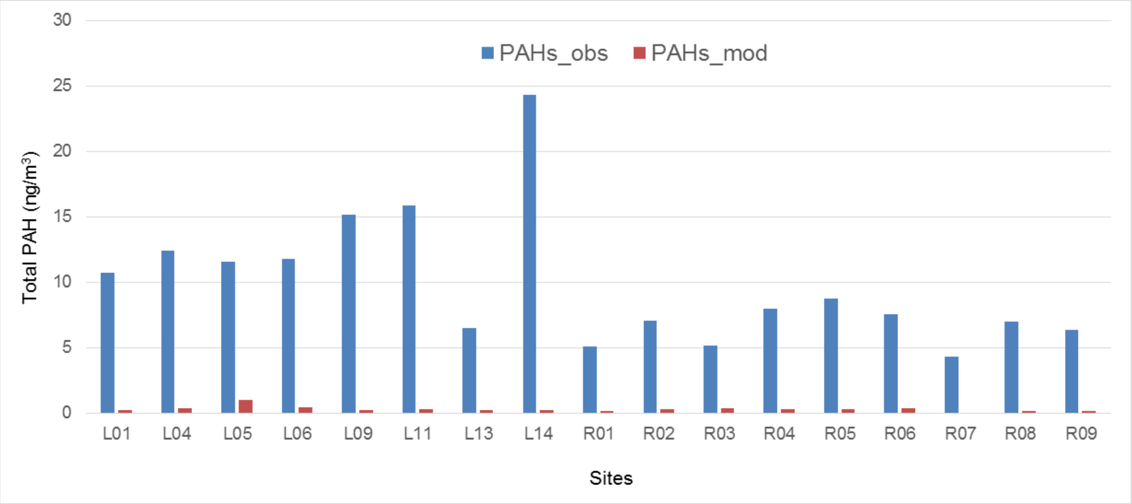

Figure S5. Model sensitivity analysis on the impact of point and line (transportation) source emissions (PAHs_mod) on total PAH concentrations at 17 passive sampling sites (PAHs_obs). PAHs_mod refers to the simulation where only the point and line sources were included in the model.

References in the Supplement

AESRD: Air Quality Model Guideline, 2013.

Alberta Environment (AENV): Air Quality Model Guideline, Pub. No. T/689, 2003.

CEMA: Development of a Modeling Emissions Inventory Database for the Implementation of Emissions Management Frameworks, available at: http://library.cemaonline.ca/ckan/dataset/2011-0038, 2011.

Environment and Climate Change Canada (ECCC) and Alberta Environment and Parks (AEP): Joint Oil Sands Monitoring Program Emissions Inventory Compilation Report, June 2016, available at: http://aep.alberta.ca/air/reports-data/air-emissions-inventory.aspx, 2016.

ECCC: Source Emissions, Oil Sands Region, Emissions-package, 2016. http://donnees.ec.gc.ca/data/air/monitor/source-emissions-monitoring-oil-sands-region/source-emissions-oil-sands-region/emissions-package/?lang=en, 2016.

Galarneau, E., Makar, P. A., Zheng, Q., Narayan, J., Zhang, J., Moran, M. D., Bari, M. A., Pathela, S., Chen, A., and Chlumsky, R.: PAH concentrations simulated with the AURAMS-PAH chemical transport model over Canada and the USA, Atmos. Chem. Phys., 14, 4065-4077, 2014.

Lott, R. A.: Case Study of Plume Dispersion Over Elevated Terrain, Atmos. Environ., 18, 125-134, 1984.

Malm, W. C.: Spatial and Seasonal Patterns and Temporal Variability of Haze and Its Constituents in the United States. Report III, Prepared by the Cooperative Institute for Research in the Atmosphere, Colorado State University, ISSN 0737 to 5352-47, 2000.

NASA: MODIS Collection 6 NRT Hotspot / Active Fire Detections MCD14DL, DOI: 10.5067/FIRMS/MODIS/MCD14DL.NRT.006, 2017.

New Zealand Ministry for the Environment: Good Practice Guide for Atmospheric Dispersion Modelling, ISBN 0-478-18941-9, 2004.

Nopmongcol, U., Jung, J., Zagunis, J.,Shah, T., Morris, R., Pollock, T.,Allan, W., Qiu, X., Walters, N., and Yang, F.: Capital Region Particulate Matter Air Modelling Assessment Final Report, available at: https://open.alberta.ca/dataset/capital-region-particulate-matter-air-modelling-assessment-final-report, 2014.

Schuster, J. K., Harner, T., Su, K., Mihele, C., and Eng, A.: First Results from the Oil Sands Passive Air Monitoring Network for Polycyclic Aromatic Compounds, Environ. Sci. Technol., 49, 2991–2998, 2015.

Scire, J. S., Robe, F. R., Ferneau, M. E., and Yamartino, R. J.: A User’s Guide for the CALMET Meteorological Model, Earth Tech Inc., January 2000, p 332, 2000.

Simon, H., Beck, L., Bhave, P. V., Divita, F., Hsu, Y., Luecken, D., Mobley, J. D., Pouliot, G. A., Reff, A., Sarwar, G., and Strum, M.: The development and uses of EPA’s SPECIATE database, Atmos. Pollut. Res., 1(4), 196-206, 2010.

US EPA: User’s Guide to the Building Profile Input Program, EPA-454/R-93-038, 1995.

US EPA: Revision to the Guideline on Air Quality Models: Adoption of a Preferred General Purpose (Flat and Complex Terrain) Dispersion Model and Other Revisions, Final Rule (40 CFR Part 51), 2005.

US EPA: Speciate 4.5, available at: https://cfpub.epa.gov/speciate/, 2017.

Vijayaraghavan, K., Nopmongcol, U., Grant, J., Morris, R., Pollock, T., Davies, M., and Person, R.: Protocol for updating and preparing a modelling emission inventory, Cumulative Environmental Management Association, Fort McMurray, Alberta, Canada, available at: http://library.cemaonline.ca/ckan/dataset/2010-0031/resource/8f449c5d-3129-4d6f-a530-46ec33a46208, 2010.